Cell cycle-coordinated maintenance of the Vibrio bipartite genome

Théophile Niault, Jakub Czarnecki, Morgan Lambérioux, Didier Mazel, Marie-Eve Val

CELL-CYCLE COORDINATED MAINTENANCE OF THE *VIBRIO* BIPARTITE GENOME

Théophile Niault[1,2 *], Jakub Czarnecki[1 *], Morgan Lambérioux[1,2], Didier Mazel[1‡] and Marie-Eve Val[1‡]

[1] Institut Pasteur, Université Paris Cité, CNRS UMR3525, Bacterial Genome Plasticity Unit, F-75015 Paris, France

[2] Sorbonne Université, Collège Doctoral, F-75005, Paris, France

* These authors contributed equally to this work

‡ Corresponding authors : marie-eve.kennedy-val@pasteur.fr , didier.mazel@pasteur.fr

RUNNING TITLE

Vibrio Bipartite Genome Maintenance

KEYWORDS

Iteron, plasmid, chromosome, multipartite, replication, segregation, *Vibrio*, DnaA, RctB, initiation

TABLE OF CONTENTS

ABSTRACT

To preserve the integrity of their genome, bacteria rely on several genome maintenance mechanisms that are coordinated with the cell cycle. All members of the *Vibrio* family have a bipartite genome consisting of a primary chromosome (Chr1) homologous to the single chromosome of other bacteria such as *Escherichia coli* and a secondary chromosome (Chr2) acquired by a common ancestor as a plasmid. In this review, we present our current understanding of genome maintenance in *Vibrio cholerae*, which is the best studied model for bacteria with multipartite genomes. After a brief overview on the diversity of *Vibrio* genomic architecture, we describe the specific, common, and coordinated mechanisms that control the replication and segregation of the two chromosomes of *V. cholerae*. Particular attention is given to the unique checkpoint mechanism that synchronizes Chr1 and Chr2 replication.

INTRODUCTION

Bacteria use sophisticated mechanisms to maintain the integrity and stability of their genomes. These mechanisms become more complex as the number of replicons increases. Bacterial genomes were long thought to be composed of a single chromosome and accessory plasmids, but the discovery of large secondary replicons of plasmid origin (i.e., megaplasmids, secondary chromosomes) in about 10% of bacteria from various lineages, has raised new questions regarding the maintenance of these genomes. A growing body of research indicates that chromosomes and large secondary replicons probably communicate to coordinate their maintenance with the bacterial cell cycle (1-7). This coordination can occur at different stages of the bacterial cycle, such as during replication, segregation, and cell division, to guarantee a proper distribution of the genetic material to the next generation.

This review article explores the bipartite genomic organization of the *Vibrio* family, with a focus on replication, segregation, and cell division in *Vibrio cholerae*, the best-studied representative of the family and the pathogen responsible for cholera. The *V. cholerae* genome consists of two essential replicons, a main chromosome (Chr1) and a secondary chromosome (Chr2). Chr2 is also sometimes called a "chromid" as it has features of both plasmids and chromosomes (8). It is believed that Chr2 was acquired by a *Vibrio* ancestor as a plasmid and coevolved with Chr1, which transferred several housekeeping genes to Chr2 (9). While most of the core genes reside on Chr1, Chr2 is enriched in species- and strain-specific genes and provides a platform for the acquisition of new adaptive functions (10). Each chromosome has its own replication system. Chr1 is initiated by the universal bacterial chromosome replication initiator DnaA, while Chr2 is initiated by the initiator RctB, which shares structural similarities with iteron plasmid initiators. Despite using distinct initiators, Chr1 and Chr2 have evolved by incorporating a unique checkpoint mechanism that allows them to communicate to coordinate their replication. At the segregation level, Chr1 and Chr2

use both specific players, such as their own ParAB partition machineries, to segregate the chromosome origins along the cell length, and common actors, such as the FtsK DNA translocase, which segregates the chromosome termini across the closing septum during cell division. In this review, we provide a comprehensive understanding of the mechanisms that evolved to maintain the bipartite genome of *V. cholerae* through comparisons with the well-studied *E. coli* chromosome and iteron plasmids.

ORGANIZATION OF *VIBRIO* GENOMES

The *Vibrionaceae* family exhibits a conserved bipartite genome organization (Fig. 1, Table S1), with Chr1 ranging in size from 2.5 Mb to 4.3 Mb (median = 3.3 Mb) and Chr2 from 0.6 Mb to 2.5 Mb (median = 1.7 Mb) (Table S2). This level of conservation is particularly high compared to other bacteria with multipartite genomic architecture, where the presence of secondary replicons is usually conserved within a single genus (8, 11). The high conservation of the bipartite genome throughout the *Vibrionaceae* family suggests that this genomic architecture is under positive selection. In *V. cholerae* species, Chr1 and Chr2 are relatively smaller (about 3Mb and 1 Mb respectively) compared to the rest of the *Vibrionaceae* (Table S2). There are also a few known examples of mono-chromosomal strains of *V. cholerae* resulting from a fusion between Chr1 and Chr2 (12-14). The reason for the stability of these fusions in a natural environment is puzzling, especially since under laboratory conditions, when chromosome fusions have been obtained to compensate for a Chr2 replication defect, they tended to spontaneously reverse to a bipartite genome configuration via the acquisition of compensatory mutations (15). Similar examples of natural fusion between large replicons have been reported in other bacteria with multipartite genomes – *Sinorhizobium meliloti* (16), *Agrobacterium tumefaciens* (17) and *Cupriavidus necator* (18).

The genetic information of the *Vibrionaceae* is not equally distributed between Chr1 and Chr2. The pangenome of 124 complete *Vibrionaceae* genomes shows that most of the core

genes are located on Chr1, while Chr2 contains more species- and strain-specific genes (19). This imbalance in gene content is also found in other multipartite bacteria (8). Chr2 can be seen as an adaptive platform into which new genes can be incorporated without disrupting the conserved organization of Chr1 (10). As in other bacteria, *V. cholerae* Chr1 has been shown to be organized in a manner that provides the highest fitness. This organization is due, at least in part, to the way Chr1 is replicated (20). Chr1 has been shown to carry more growth rate-related genes, such as the rRNA operon and ribosomal genes, close to its replication origin (19, 21). This may be partly explained by the fact that the products of these genes are in increased demand under rapid growth conditions, when multiple simultaneous replication rounds occur, increasing the dosage of genes lying around the *ori1* (21). However, it has been proposed that this organization is also important under free-growth conditions, indicating that it may have evolved for reasons that are independent of gene dosage, such as the importance of the localization of the expression of certain genes in the cell (which is due to the specific localization of particular Chr1 fragments) or the effect of their expression on the overall fluidity of the cytoplasm (22, 23).

In addition to the bipartite core genome, *Vibrionaceae* strains carry a highly variable set of plasmids that are not essential for host cell growth, but may have some adaptive functions (Fig. 1) (8, 24). Interestingly, when comparing plasmid abundance in *Vibrionaceae* and *V. cholerae*, we observe a much lower presence of plasmids in the latter (Table S2). This is due to a sub-branch of *V. cholerae*, the El Tor type, which has been extensively sequenced because of its prominent role in cholera epidemics and which does not carry plasmids. The absence of plasmids in *V. cholerae* El Tor is due to the presence of defense systems located in two genomic islands (*Vibrio* pathogenicity island 2, VPI-2, and *Vibrio* seventh pandemic island II, VSP-II) that render plasmids unstable and eliminate them from the population (25).

REPLICATION OF THE BIPARTITE GENOME OF *V. CHOLERAE*

157 *V. cholerae* El Tor N16961 is one of the most studied members of the *Vibrionaceae* family,
158 and its genome was one of the first to be sequenced (26). It consists of a 2.96 Mb Chr1 and
159 a 1.07 Mb Chr2. Distinct mechanisms initiate replication of Chr1 and Chr2. Chr1 follows a
160 chromosome-like initiation process, while Chr2 has an initiation mechanism similar to that
161 found in iteron plasmids (27, 28). Despite their difference, both chromosomes replicate in a
162 coordinated manner (7). This intriguing observation in *V. cholerae* led to its extensive study
163 to better understand the mechanisms that govern the coordinated replication of its two
164 chromosomes.

165 **Chr1 replication initiation control is analogous to that of the *E. coli* chromosome.**

166 **Chr1 origin of replication.** Chr1 replication is initiated by the universal bacterial initiator
167 DnaA, as is the case for *E. coli* chromosome replication. The Chr1 replication origin (*ori1*) in
168 *V. cholerae* shares a significant level of sequence identity (58%) with the replication origin of
169 the *E. coli* chromosome (*oriC*) (Fig. 2). Both origins contain five strong DnaA boxes, an AT-
170 rich region and an IHF box. Furthermore, the DnaA proteins of *V. cholerae* ($DnaA_{Vc}$) and *E.*
171 *coli* ($DnaA_{Ec}$) show a high level of amino acid identity (79%). In fact, a plasmid carrying *ori1*
172 can replicate in *E. coli* (28), and *ori1* can effectively replace *oriC* in the *E. coli* chromosome
173 (29, 30). These results reveal that the $DnaA_{Ec}$-*oriC* and $DnaA_{Vc}$-*ori1* systems are functionally
174 interchangeable.

175 In *E. coli*, several regulatory mechanisms work together to ensure adequate initiation of
176 chromosome replication at all growth rates (31, 32). While these pathways have not been
177 directly studied in *V. cholerae*, many are thought to be present based on the presence of
178 homologs of key regulatory genes and DNA sequences in its genome. However, certain
179 variations exist, such as the absence of a homolog of Hda in *V. cholerae* and differences in
180 the stringent response. These aspects are discussed in more detail in the subsequent
181 sections.

Post-initiation inactivation of *ori1* by SeqA. Both *E. coli oriC* and *V. cholerae ori1* are characterized by an overrepresentation of GATC motifs (Fig. 2A) (29, 30). Like *E. coli*, *V. cholerae* contains the Dam methylase that methylates the adenine of the GATC motif throughout the genome (33). Following the passage of the replication fork, GATC motifs become transiently hemi-methylated and are specifically recognized by the SeqA protein. In *E. coli*, SeqA binding at *oriC* prevents immediate replication re-initiation by impeding the recruitment of DnaA (34). In *V. cholerae*, the deletion of *seqA* leads to over-initiation of replication at *ori1*, indicating a similar role to that of SeqA in *E. coli* (29).

DnaA inactivation. DnaA exists in two nucleotide-bound forms: DnaA-ADP and DnaA-ATP. DnaA-ATP is the active form of the protein and is responsible for the initiation of DNA replication. DnaA-ADP is the inactive form and has a lower affinity for DNA. The switch from DnaA-ATP to DnaA-ADP is critical to regulate chromosome initiation (31). In *E. coli*, the Regulatory Inactivation of DnaA (RIDA) is facilitated by the interaction of DnaA with ATP-bound Hda (homologous to DnaA) (35). It is unclear whether RIDA occurs in *V. cholerae* as it does in *E. coli*, given that no homologue of Hda has been identified (27). In *E. coli*, the second system of direct inactivation of DnaA involves its binding to a specific chromosomal region called *datA* (*datA*-dependent DnaA-ATP hydrolysis, DDAH) (36). *V. cholerae* Chr1 harbors a putative analog of the *datA* site, located within the same genomic context as the *orn* (VC0341) and *queG* (VC0342) genes. In *E. coli*, together the two systems RIDA and DDAH prevent *oriC* over-initiation by rapidly converting the free DnaA-ATP pool to DnaA-ADP. It is possible that in *V. cholerae*, DDAH has a more prominent role in overcoming the absence of RIDA, or an as-yet-unknown mechanism may substitute for RIDA. Since RIDA is one of the primary mechanisms for the conversion of DnaA-ATP to DnaA-ADP in *E. coli*, it will be important to understand how DnaA inactivation occurs in *V. cholerae*.

DnaA regeneration. When replication progresses and cell volume increases, the batch of DnaA-ADP is progressively converted back to DnaA-ATP, to allow further initiation. DnaA-ATP is exclusively produced through the passive binding of free DnaA proteins to ATP, which

209 is abundantly present in the cytosol. Three mechanisms for the production of free DnaA
210 protein have been identified: *de novo* translation of DnaA, DnaA-ADP dissociation stimulated
211 by interaction with membrane phospholipids, and binding to chromosomal sites called DnaA-
212 Reactivating Sequences (DARS1 and DARS2) (31). When these sites are replicated, they
213 double in copy number, leading to an acceleration in the rate of DnaA-ATP formation. Hence,
214 the positioning of these sites on the genome is crucial and relocating them to other loci alters
215 the regulation of *oriC* initiation (37). In *V. cholerae*, two DARS analogues, DARS1 and
216 DARS2, are located at the same positions as in *E. coli*, at the *uvrB* and *mutH* promoters on
217 Chr1 (Fig. 2B) (38).

218 **Other regulatory mechanisms.** *E. coli* and *V. cholerae* potentially share additional
219 mechanisms to regulate DnaA activity and ensure the timely initiation of chromosomal
220 replication during the cell cycle. In *E. coli*, the protein DiaA acts as an accessory factor,
221 facilitating the loading of DnaA onto *oriC* by interacting with DnaA and promoting the
222 formation of an active DnaA-ATP complex (39, 40). In *V. cholerae*, a DiaA/GmhA homolog
223 encoded by VC0579 contains the L190 and F191 residues in its C-terminal domain, which
224 are essential for interacting with DnaA in *E. coli* (39). Another phenomenon observed in both
225 *E. coli* chromosome and *V. cholerae* Chr1 is the arrest of replication during amino acid
226 starvation, also known as the stringent response. The increase in intracellular (p)ppGpp
227 levels activates the Lon protease, which specifically degrades DnaA-ADP, inhibiting
228 replication initiation (41, 42). During the activation of the stringent response, replication forks
229 that have already formed can complete genome replication. This phenomenon can be used
230 to synchronize cell populations by inducing stringent response with a serine analogue (serine
231 hydroxamate - SHX) in both *E. coli* and *V. cholerae* (42, 43). Curiously, *E. coli* and *V.*
232 *cholerae* do not respond similarly to the induction of the stringent response. In *E. coli*, under
233 SHX treatment, new rounds of initiation are blocked, the cells complete their replication but
234 do not divide, resulting in cells with two sets of complete genomes. *V. cholerae* behaves
235 differently. Firstly, cell division is not inhibited by SHX. Moreover, after SHX treatment the

replication process follows three stages: an initial shutdown phase, a restart phase, and a final shutdown phase. During the first stage, initiation is blocked, the cells complete their replication and divide. Then, cells re-initiate replication once (second stage), complete it and ultimately divide (final stage). The end result is daughter cells containing a single set of genomes (44). These differences suggest a distinct mechanism of stringent response in *V. cholerae* compared to *E. coli*, which would deserve further study.

The control of Chr2 replication initiation resembles that of iteron plasmids but also involves additional coordination with the cell cycle.

Chr2 origin of replication. Chr2 contains a replication origin (*ori2*) similar to that found in iteron plasmids, a class of autonomous genetic elements frequently carrying antibiotic resistance genes and virulence factors. Iteron plasmids are named after their repetitive and directed sequences known as iterons, which are organized into an array located at the origin of replication. Examples of well-known iteron plasmids include RK2, F, R6K, P1, pPS10, and pSC101 (45). The number of iteron sites in the array can vary, with at least three in ori_{pSC101} and up to seven in ori_{R6K} (Fig. 3). The size of iterons also varies, ranging from 17 bp for ori_{RK2} to 22 bp for ori_{R6K}. Iteron plasmids encode an initiator protein, typically called "Rep," located near their origin. Rep proteins bind to the iteron array and introduce torsional forces that facilitate melting of the double-stranded DNA helix at an adjacent AT-rich region known as the DNA Unwinding Element (DUE) (46). The iteron origins contain binding sites for host factors important for replication initiation, such as DnaA and IHF (46). In addition, the Rep protein binds to its own promoter as a dimer on an operator formed of inverted iteron repeats. This causes a negative feedback loop limiting the number of Rep proteins in the cell (47, 48). Some iteron plasmids may contain an *inc* region ("incompatibility" region) that contains additional iteron repeats, which are not directly involved in DNA unwinding but regulate replication initiation (Fig. 3).

261 The organization of *ori2* in Chr2 resembles that of iteron plasmids. Chr2 encodes its own
262 initiator protein, RctB, next to the origin. *ori2* harbors an array of six regularly spaced iterons
263 (12-mer), a DUE, a DnaA box and an *inc* region containing additional iterons. Unlike plasmid
264 iterons, all iterons in *ori2* have a built-in GATC motif that must be fully methylated by Dam
265 methylase in order to be bound by RctB (29). Furthermore, RctB binds to a second type of
266 sites that has no similarity to iterons, called 39-mer (39m) or 29-mer (29m) depending on
267 their size (49, 50). These sites have a negative regulatory role on *ori2* initiation. They are not
268 found in plasmids but conserved in all *Vibrionaceae* Chr2. Two 39m sites are located in the
269 *inc* region and the 29m site is in the *rctB* promoter (Fig. 3). RctB is thought to bind to the
270 29/39m as a dimer forming a dyadic structure, but direct experimental evidence is lacking as
271 there is no published structure of RctB on DNA. 29/39m contain GC-rich imperfect direct
272 repeats at their ends with an AT-rich intermediate sequence. The GC-rich repeats, which are
273 recognized by RctB, are on the same side of the DNA helix (49). The 29m site contains an
274 internal deletion of 10 nt, causing a complete rotation of the DNA helix that does not disrupt
275 the phasing of the two GC-rich repeats (49). Importantly, unlike the iterons, RctB binding to
276 29/39m is not influenced by their methylation, as they do not contain GATC motifs.

277 **Comparison of RctB with Rep initiators from iteron plasmids.** The large majority of
278 iteron plasmid replication initiators (Reps) are proteins of about 300 amino acids long and
279 typically composed of two domains, WH1 and WH2 (Fig. 4 A-C). Each of these domains
280 contains a winged helix-turn-helix motif that participates in iteron binding. RctB, with its 658
281 residues, is twice the size of Reps and is divided into four structural domains (I to IV) (51).
282 Domain II (aa 182-360) and domain III (aa 361-472) of RctB were crystallized together to
283 form a stable segment of approximately 38 kDa (52). Both of these domains contain a HTH
284 motif required for DNA binding and are structurally homologous to the WH1 and WH2
285 domains of Rep initiator proteins (pi, RepE, RepA) (Fig. 4 D). In solution, the Reps exist as a
286 dimer, in which the interaction occurs between the WH1 domains in a head-to-head
287 arrangement. The crystal structure of RctB (domains II-III) reveals that the interaction surface

288 within the RctB dimer is located between domains II (52). The dimeric head-to-head
289 organization of Reps and RctB, however, is not consistent with the organization they must
290 adopt when cooperatively binding to the iteron array. In fact, Reps and RctB are active for
291 initiation through their monomerization which is performed by DnaK/J chaperones (53, 54).
292 RctB interacts with DnaK at the K-I site, extending from residues 150 to 163 (55). In the case
293 of Reps, monomerization can also be achieved when the Rep dimer interacts with an iteron
294 (56). Whether RctB is monomerized upon DNA binding is unknown.

295 As already mentioned, RctB contains two additional domains, domain I and IV, located,
296 respectively, at the N- and C-terminus of the protein's conserved core (Fig. 5 A-B). Domain I
297 contains a winged HTH DNA-binding motif involved in iteron binding. This domain is
298 essential for the initiation of replication at *ori2*. In the model proposed by Orlova *et al.* (52),
299 domain I and domains II-III bind to opposite surfaces of the iteron, with domain I and domain
300 II binding directly to the iteron and domain III binding to adjacent sequences in a non-specific
301 manner (Fig. 5 C-D). Acquisition of an additional N-terminal DNA-binding domain has been
302 observed in some Reps, such as TrfA from the RK2 plasmid. Its additional N-terminal DNA-
303 binding domain (DBD), is analogous to the domain I of RctB, and is essential for interaction
304 with iterons (57).

305 Unlike domain I, domain IV is not essential for replication initiation, but is involved in Chr2
306 copy number down-regulation (51, 53, 58). So far, the crystal structure of the domain IV has
307 not been published. However, modeling shows that it does not resemble any known structure
308 and is only found in proteins closely related to RctB. The domain IV plays a central role in the
309 negative regulation of *ori2* (51). Although it lacks a DNA-binding domain, domain IV is
310 essential for binding to 29/39m (51). The same domain IV was shown to promote self-
311 interaction with other RctB. This suggests that two RctB monomers can interact not only
312 through domain II, but also through domain IV. Mutations that disrupt interactions through
313 domain IV also prevent RctB from binding to 29/39m sites (51). This suggests that binding of
314 29/39m may require dimerization of RctB through domain IV.

Chr2 replication initiation. The minimal *ori2* (*ori2*min) is a compact region of DNA containing numerous regulatory sequences. The *ori2*min consists of six regularly spaced iterons, a DnaA box, an IHF binding site (IBS), and an AT-rich region (DUE). Upon binding of RctB to the iterons, unwinding of the DNA duplex occurs in the DUE region (Fig. 6A). The organization and function of the *ori2*min region are under strict constraints, since neither the position nor the orientation of these regulatory sites can be changed, nor can the sequence and spacing of the iterons. Only one iteron can be inactivated at a time, and some cannot be inactivated at all (59). Both the DnaA-box and the IBS are also essential for Chr2 replication (59). To promote replication initiation at *ori2*, RctB binds cooperatively to the six-iteron array and simultaneously to the DUE lower strand, forming a ternary complex (60). The DUE contains six regularly spaced direct tetra-nucleotide repeats of 5'-ATCA recognized by RctB. Formation of the ternary complex requires the binding of the IHF protein downstream of the iteron array, which causes a 180° bend in the DNA. This bending results in the opening of DNA at the two ATCA sites closest to the IBS (Fig. 6B) (60). The mechanism of DNA duplex unwinding by RctB is analogous to that of DnaA (61, 62). In both cases, the initiator protein oligomerizes on double-stranded DNA and interacts with the single-stranded DNA of the DUE (Fig. 6B). DnaA interacts with single-stranded DNA through the H/B motif (V211 and R245 residues) contained in its domain III (63, 64). The region within the RctB protein that mediates the interaction with ssDNA is still unknown. The subsequent steps involving replisome recruitment and assembly will be covered in the upcoming section titled "Post-initiation replication stages in *V. cholerae*"

Control of Chr2 replication initiation - similarities to iteron plasmids.

Iteron plasmids can be present inside the cell at medium to low copy number, so their maintenance requires tight regulation of replication. There are four main mechanisms for regulating initiation: autoregulation of the *rep* gene, titration of the initiator, dimerization of the Rep protein, and origin handcuffing. These mechanisms have been thoroughly reviewed in (46, 65-67).

342 The mechanisms of titration and autoregulation involve regulating the amount of Rep
343 available in the cytoplasm. Plasmids contain iteron sites that are not essential for replication
344 but that regulate the pool of Rep proteins. In many iteron plasmids, the Rep promoter
345 contains an operator site consisting of two inverted iterons (Fig. 3). In this arrangement, Rep
346 proteins bind as dimers, obstructing access for RNA polymerase (47, 68-70). This creates a
347 negative autoregulatory loop to produce Rep protein at the appropriate level for controlled
348 initiation. Similarly, Chr2 exhibits autoregulation through a feedback loop of *rctB* expression
349 (50), which does not rely on inverted iteron repeats but on the 29m site (Fig. 3), which
350 coincides with the *rctB* mRNA transcription start site, spanning from position -4 to +25 (50).
351 Another crucial mechanism regulating replication initiation is the existence of Rep as free
352 dimers. The dimeric form is considered inactive for initiation since Rep dimers bind less
353 efficiently to iterons (71). Rep must be monomerized by chaperones to become active (54,
354 72). As mentioned earlier, RctB also exists as an inactive dimer and is converted into an
355 active form through monomerization mediated by DnaK/J chaperones (53, 55, 58). It remains
356 uncertain whether DNA binding triggers RctB monomerization as for Rep.
357 The final mechanism involves inactivation of the origin through DNA bridging by Rep
358 proteins, known as "handcuffing". This process occurs when Rep proteins bound to the iteron
359 array interact with Rep proteins bound to other sites, preventing replication initiation by steric
360 hindrance (73, 74). Rep proteins can either interact with Rep bound to the same sites on
361 different plasmids (intermolecular handcuffing) or to different iterons within the same plasmid
362 (intramolecular handcuffing). For instance, in the plasmid pPS10, RepA proteins bound to a
363 four-iteron array of a plasmid can interact with those of another plasmid. This intermolecular
364 handcuffing prevents replication initiation when the copy number of pPS10 increases (75). In
365 plasmid F, RepE mediates handcuffing between iterons in the *ori* region and iterons in the *inc*
366 region. This intramolecular handcuffing causes DNA looping, leading to inhibition of
367 replication initiation (76, 77). In the case of Chr2, intermolecular handcuffing is unlikely to
368 regulate initiation due to the immediate segregation of newly replicated *ori2* at two distant
369 locations in the cell (see section on origin segregation). Thus, similar to the F plasmid,

intramolecular handcuffing within *ori2* must occur. However, this mechanism must differ from the bridging between iterons from the *inc* region and the *ori2*min region. The *inc* region of Chr2 contains five regulatory iterons. When these iterons are inactivated, the copy number of *ori2*-driven plasmids decreases, indicating that these iterons play a positive role in the initiation of Chr2 replication, contrary to the iterons in the *inc* region of plasmid F (49). Therefore, it has been proposed that Chr2 handcuffing is dependent on RctB bound to the 39m also present in the *inc* region (49, 53). One may wonder why *ori2* acquired a new type of binding sites for RctB (29/39m), when iteron plasmids already have very tight control over their replication. For example, the F plasmid is maintained very stable in the population with a copy number of 1 per cell, while it contains only one type of binding sites for Rep. The 29/39m could therefore be a functional innovation on *ori2* that would have led to the emergence of replication coordination between Chr1 and Chr2. This will be discussed later.

Regulation of Chr2 replication initiation - similarities to that of the main chromosome.

Chr2 has additional levels of regulation of replication initiation that resemble those of Chr1. The first mechanism links Chr2 replication initiation to DNA methylation status. Like Chr1, Chr2 harbors an overrepresentation of GATC motifs in its origin. The binding of SeqA at the hemi-methylated *ori2* prevents immediate re-initiation (29). As for *ori1*, the absence of *seqA* provokes an over-initiation at *ori2* (29). Interestingly, most iteron plasmids do not show enrichment for GATC motifs in their origin. The exception is plasmid P1, where full Dam methylation of GATC sites located near iterons is essential for replication as it facilitates DNA unwinding at the DUE (78-80).

In addition to SeqA hindering *ori2* re-initiation, another control by Dam methylation occurs at *ori2*. RctB is only able to bind to fully Dam-methylated iterons (29). In the absence of Dam, Chr2 initiation is therefore impossible, resulting in cell death (81). The only way to rescue a *dam*-deleted mutant is through spontaneous fusion of Chr2 into Chr1 so that it can benefit from the replicative machinery of Chr1 (81).

A second mechanism that makes Chr2 regulation related to that of main chromosomes is the existence of titration sites for the replication initiator. Chr2 has six RctB binding sites (five iterons and one 39m motif) in a region spanning 74 kb near *ori2*. These loci are duplicated early after Chr2 replication initiation and negatively regulate re-initiation by binding RctB molecules (82).

crtS-mediated synchronization of Chr1 and Chr2 replication termination

Replication termination of Chr1 and Chr2 is synchronized. Chr1 and Chr2 are replicated once per cell cycle (83). Overlapping rounds of replication can occur under conditions of rapid growth, resulting in amplification of regions around the origins, however termination of replication occurs only once per cell cycle for both chromosomes (84). Chr1 and Chr2 follow a sequential initiation choreography. Chr1 is initiated first and when it is 2/3 replicated, Chr2 initiates replication (7). Since Chr2 is about one-third the size of Chr1, the two chromosomes complete replication synchronously. Synchronous termination of Chr1 and Chr2 replication appears to be an evolutionarily selected trait in the *Vibrionaceae* (42).

The regulation of *ori2* by Dam methylation, by handcuffing with 39m, or by *rctB* autorepression may explain how Chr2 replication is limited to once per cell cycle but does not explain how Chr2 replication is timed to Chr1 replication. A new layer of regulation was uncovered, directly linking Chr1 replication to Chr2 replication.

The *crtS* site coordinates Chr1 and Chr2 replication. In 2014, Baek *et al.* performed a ChIP-on-chip experiment with RctB and discovered additional binding sites outside of *ori2* (82). Among them, RctB bound in an intergenic region of two co-directional non-essential genes, VC0764 (predicted function of alanyl-tRNA synthetase) and VC0765 (homolog of *yfgJ* ECOLI:G7318 in *E. coli*, no known function) located on the right arm of Chr1, 690 kb downstream of *ori1*. This region does not contain any known RctB binding sequence (i.e. iteron and 29/39 m). This RctB binding region was found to have an enhancing effect on *ori2* initiation and, when placed in *trans* on a plasmid, increased Chr2 copy number (82). In 2016,

Val *et al.* demonstrated that this site acts as a timer that triggers the initiation of Chr2 upon replication on Chr1 (15). They showed that when the Chr1 RctB binding site was moved near *ori1*, Chr2 replicated earlier and when it was moved near *ter1* (terminus of Chr1), Chr2 replicated later in the cell cycle (Fig. 7). The site was therefore named *crtS* for Chr2 replication triggering Site (15). Based on marker frequency analysis (MFA), there is a constant delay between *crtS* replication and *ori2* triggering, which corresponds to the replication of ~200 kb (Fig. 7), probably due to the time required to recruit and assemble the replisome.

The sequence of *crtS* is conserved with a shared synteny in all *Vibrionaceae* genomes and the distance between *crtS* and *ter1* is correlated with the size of Chr2 (42). The evolutionary selection of *crtS* location on the main chromosome ensures the simultaneous termination of replication of both chromosomes in all *Vibrionaceae* (42). Why is synchronizing the end of replication of Chr1 and Chr2 an evolutionary choice? Could it serve as a backup mechanism that allows correct segregation of the two chromosomes in coordination with cell division? In mutants where *crtS* is displaced on Chr1 and replication termination of the two chromosomes is no longer synchronous, no growth defects was observed under laboratory conditions (15). However, it would be necessary to test the growth of these mutants in conditions closer to their natural environment.

The *crtS* locus controls not only the timing of initiation, but also the number of Chr2 copies. By adding more copies of *crtS* in the *V. cholerae* genome, the number of Chr2 copies gradually increases (85). *crtS* is also active in *E. coli* and can regulate the copy number of an *ori2*-driven plasmid (82, 85). This finding offers the capacity to manipulate the dosage of genes of interest encoded on an *ori2*-driven plasmid by modifying the *E. coli* host with various numbers of *crtS* sites (85).

Successive deletion experiments demonstrated that the minimum size of *crtS* is 62 bp (85). In *crtS*-deleted mutants, time-lapse fluorescence microscopy reveals sporadic and infrequent

instances of Chr2 initiation (15). Although not absolutely essential under laboratory conditions, the deletion of *crtS* results in a filamentous phenotype, severely impaired growth, and DNA damage (15). Δ*crtS* mutants are therefore unstable and prone to mutations, such as genome rearrangements like chromosome fusion, as well as the acquisition of compensatory mutations in the *rctB* gene or in *ori2* (15, 51).

Mechanism of action of *crtS* on *ori2*. The precise mechanism underlying *crtS* role in the initiation of Chr2 replication remains unclear, raising two key questions: (1) How does *crtS* become activated to initiate replication at *ori2* after passage of the replication fork? (2) What molecular events occur at *ori2* when *crtS* has replicated?

(1) *crtS* activation upon replication. The passage of a replication fork through a DNA locus can have many consequences. The most obvious is the doubling of its copy number. The replicated locus also transitions from a fully methylated to a hemi-methylated state, which is important for many replication-related mechanisms, such as blocking re-initiation at *oriC* or DNA mismatch repair (86). Replication also induces changes in DNA topology, such as the formation of positive supercoiling upstream of the replication fork (87). Replication forks can also transiently remove DNA-binding proteins (88). Finally, replication promotes the structuring of single-stranded hairpins between Okazaki fragments (89). Some of the consequences of replication fork transitions have been tested for *crtS*.

The *crtS* locus is flanked by several GATC methylation sites. Since RctB binding is sensitive to the methylation state of the iterons, the methylation state of *crtS* could also be important for RctB binding at this locus. However, mutation of the GATC sites in the vicinity of *crtS* had no effect on its activity (85).

Further studies have shown that *crtS* duplication alone could be sufficient to send a replication initiation signal to *ori2* (15, 85, 90). Ramachandran *et al.* set up a system allowing them to block the replication of Chr1 (by flanking *ori1* by the Ter/*tus* replication fork trap) and showed that two unreplicated copies of *crtS* are able to increase Chr2 copy number in a

474 subpopulation of cells which suggests that *crtS* gene dosage may be a sufficient signal to
475 trigger Chr2 initiation (90).

476 Ciaccia *et al.* have discovered that the global regulator Lrp (Leucine Responsive regulatory
477 Protein) binds to *crtS* (91). *crtS* contains in its 5' part the AT-rich sequence
478 TAGATTTATTCTT very close (12/15 nucleotides) to the Lrp binding site consensus
479 (YAGHAWATTWTDCTR, (92)). In the Δ*lrp* strain, the *crtS* site does not function, and Chr2 is
480 under-replicated. *In vitro*, Lrp facilitates the binding of RctB to *crtS*. Lrp is known to form a
481 nucleosome-like structure which wraps DNA. This local DNA conformational change could
482 allow RctB to recognize the *crtS* site (93). In this aspect, *crtS* is analogous to DARS-2 in *E.*
483 *coli*, which requires the binding of two Nucleoid Associated Proteins (NAPs), Fis and IHF, to
484 regenerate DnaA-ATP (94). Moreover, Fis binding to DARS2 was recently shown to fluctuate
485 during the cell cycle, which is important for coordinating replication initiation (95). Perhaps
486 just as Fis is key to DARS-2 function, Lrp may be key to sensing replication fork crossing
487 through *crtS*. Lrp has already been shown to sense fork crossing in some cases (96). Further
488 research on *crtS* regulation by Lrp is needed.

489 **(2)** <u>*ori2* activation post-*crtS* replication.</u> Val *et al.* gained significant insights into the
490 mechanism of *ori2* activation by *crtS* by studying a mutant called $crtS_{WT}/_{VC23}$, which contains
491 two chromosomal copies of *crtS* located at distant positions (15). In this mutant, an additional
492 copy of *crtS* is located near *ori1*, in addition to the native locus. Using fluorescence
493 microscopy to observe cells tagged at *ori2*, they discovered that daughter cells were born
494 with two *ori2*, then progressed through a three *ori2* stage, and finally reached a four *ori2*
495 stage before undergoing cell division. This sequential activation of *ori2* replication suggests
496 that the duplication of a single *crtS* site activates a single *ori2*, implying that *crtS* exerts a
497 localized effect (15). *In vivo,* a 3C (chromosome conformation capture) analysis revealed
498 frequent interactions between the regions surrounding *ori2* and *crtS*, suggesting that the
499 initiation of Chr2 replication may require a direct interaction between *crtS* and *ori2* (15). Baek
500 *et al.* observed that the presence of *crtS* increases the binding of RctB to iterons and

501 decreases its binding to 39m (82). They proposed a model in which *crtS* could act as a DNA
502 chaperone by remodeling RctB to alter its binding efficiency to iterons and to the 29/39m
503 sites at *ori2*. More recently, it was shown that the effect of *crtS* on *ori2* depends on the
504 presence of the 29/39m. When the 29/39m sites are mutated, replication at *ori2* proceeds
505 independently of *crtS*. Furthermore, when RctB is mutated in its domain IV (L651P mutation),
506 it no longer interacts with 29/39m and initiation at *ori2* occurs independently of *crtS* (51).
507 Another recent study showed that monomeric RctB mutants (D292R, D314P, A320R and
508 S313W/D314W) present at the dimerization interface of domain II are insensitive to the
509 presence of *crtS* (97). Perhaps the 29/39m handcuffing requires a dimeric form of RctB
510 interacting through domain II, as is the case for RepE in plasmid F (76). Structural data on
511 the 29/39m mediated handcuffing would be key to understanding the full mechanism of *crtS*.
512 All these compiled results allow us to speculate on a model of *ori2* activation by *crtS* (Fig. 8).

513 **Post-initiation replication stages in *V. cholerae***

514 **Replisome loading.** In bacteria, after DNA melting at the origin of replication, the replication
515 helicase DnaB is recruited to ssDNA. DnaB forms a ring-shaped hexameric complex. This
516 complex translocates across ssDNA in the 5′→3′ direction, separating the two DNA strands
517 before the replisome as it progresses (reviewed in (98, 99)). In *E. coli*, loading the DnaB
518 hexamer onto ssDNA requires a loading protein, DnaC, which allows the DnaB hexamer to
519 open (100). In *B. subtilis*, this process is provided by a protein called DnaI (101).
520 Interestingly, the DnaC/DnaI homologs are not present in most bacteria, including *V.*
521 *cholerae*, where their function is performed by the DciA protein. It turns out that DnaC/I
522 proteins are derived from domesticated prophages and have displaced DciA in some
523 bacterial lineages, including the most important models of Gram-negative and Gram-positive
524 bacteria, which are *E. coli* and *B. subtilis* (102). In the case of *V. cholerae ori1*, it has been
525 shown that the non-DNA-bound DnaB hexamer adopts a partially open conformation, unlike
526 that of *E. coli*, and is able to load onto ssDNA without the engagement of a loading protein.
527 Thus, the DciA protein is not necessary for DnaB loading in *V. cholerae*. However, DciA has

been shown to facilitate the loading of DnaB onto ssDNA and affect helicase activity (103, 104).

Recruitment of the helicase to *ori2* has yet to be investigated. Several scenarios of this process have been observed in iteron plasmids (reviewed in (98)). In the case of pSC101, RepA, DnaA and DnaC are co-participating in the loading of DnaB (105). In contrast, in the case of plasmid RK2 in *Pseudomonas putida*, the initiator TrfA-44 can recruit DnaB by itself ((106, 107). Further studies are needed to determine how helicase recruitment occurs after melting of *ori2* by RctB.

Replication elongation. Immediately after DnaB is loaded onto ssDNA, the rest of the replicon is assembled, comprising a DnaG primase, a clamp loader and a DNA polymerase III complex (99, 108). From their MFA profile, it appears that the replication of both chromosomes is bidirectional from *ori* to *ter* (Fig. 7) (15). Thus, it is expected that both *ori1* and *ori2* are loaded with two replisomes, working in opposite directions. MFA of *V. cholerae* in exponential phase indicates that the replication rate is constant for the whole genome and identical for Chr1 and Chr2 (15). This is expected because there are no additional genes involved in replication on Chr2, neither polymerase nor helicase, so Chr2 replication depends entirely on the machinery encoded by Chr1. Chromosome conformation capture data show physical contacts between the bottom third Chr1 and the entire Chr2 during exponential growth (15). These contacts are lost in the non-replicative stationary phase indicating that the replication machineries of both chromosomes are in close proximity until termination. Espinosa *et al.* developed a new method to capture cohesion behind replication fork named HiSC2 for High-Resolution Whole-Genome Analysis of Sister Chromatid Contacts (109). After the passage of the replication fork, the two sister chromatids remain in preferential contact in certain areas. There are five major regions of cohesion along the genome: *ori1*, *ori2*, *dif1*, *dif2* and around the pathogenicity island VPI-1. Cohesion is not related to differences in replication fork speed, nor to initiation and termination processes. Presumably, cohesion is caused by sequence specific unknown factors except for VPI-1. In that case,

555 cohesion is due to H-NS protein which extends cohesion within the VPI-1 pathogenicity
556 island and to a lesser extent on the O-antigen locus. Then, at the end of the cell cycle most
557 of the cohesion between sister chromatids are released prior to cell division, except near *dif1*
558 (109).

559 **Replication termination.** When the two replication forks reach the end of each replichore,
560 they eventually meet in the Ter regions of Chr1 and Chr2. In both *E. coli* and *B. subtilis*, there
561 is an active termination trap system, Tus/*ter* and RTP/*ter*, respectively (110). These systems
562 block fork progression to ensure termination in the Ter region. However, these systems
563 appear to have been acquired recently by horizontal gene transfer from plasmids (111). *V.*
564 *cholerae*, although closely related to *E. coli*, has no Tus or RTP homolog. It has been shown
565 that in *V. cholerae*, if the *ori* is relocated, or if an ectopic *ori* is inserted into the chromosome,
566 the point of fork convergence is shifted. This convergence point is therefore not dependent
567 on an active trapping system. Replication spontaneously terminates when two replication
568 forks meet and merge (111).

569 ## CHROMOSOME SEGREGATION AND PARTITION

570 After replication, the two copies of the bacterial genome segregate towards opposite poles,
571 allowing each daughter cell to inherit a copy of the genome after cell division. To facilitate
572 this process, various factors organize the chromosomes to ensure their proper segregation.
573 These factors have been extensively studied in *E. coli*, *C. crescentus*, and *B. subtilis*.
574 Currently, there is growing interest in studying these factors in more unconventional bacterial
575 models, such as *V. cholerae* or *A. tumefaciens* (6), where the division of the genome into
576 multiple replicons poses new questions for investigation.

577 ### Chr1 and Chr2 longitudinal arrangement

578 The organization of bacterial chromosomes can be broadly divided into two categories:
579 transversal and longitudinal arrangements (112). In the transversal arrangement, which is

that of the *E. coli* chromosome, the origin (*ori*) and terminus (*ter*) of replication are positioned in the middle of the cell at the onset of the cell cycle, while the left and right chromosome arms (replichores) are located on opposite halves of the cell. In the longitudinal arrangement, the *ori* and *ter* are located at opposite poles of the bacterium at the onset of the cell cycle, and both replichores lie along the longitudinal axis. Based on the spatial location of the *ori* in *V. cholerae*, it was thought that the arrangement of Chr1 and Chr2 in the cell might be different, since *ori1* was polar and *ori2* was located near mid-cell (113). However, a more in-depth analysis of the location of 12 loci on Chr1 and 7 loci on Chr2 revealed that both Chr1 and Chr2 are arranged in a longitudinal pattern (114). Chr1 occupies the entire cell length, with its origin (*ori1*) located at the old pole and its termination (*ter1*) at the new pole. Chr2 occupies only the younger half of the cell, with its origin (*ori2*) at mid-cell and its termination (*ter2*) located between the new pole and mid-cell (Fig. 9) (114).

Cell division control

The process of cell division in bacteria involves the formation and assembly of the divisome, a complex of proteins that are recruited to the division site during the cell cycle. The assembly of the divisome usually occurs in two stages. In *E. coli*, the initial stage, which occurs at about 25-40% of the cell cycle, begins with the FtsZ protein forming a ring-like structure called a Z-ring in the middle of the cell (115). The Z-ring is anchored to the cell membrane by a set of proteins (FtsA, ZipA) that are recruited at the same time. In a second stage, at about 50% of the cell cycle, proteins involved in cell wall remodeling and chromosome segregation (FtsK, FtsQ, FtsL, FtsB, FtsW, FtsI, FtsN) are recruited to the divisome (115). The process of septation, which separates the mother cell into two daughter cells, begins after the arrival of the second set of proteins and continues through the second half of the cell cycle. In *V. cholerae*, the timing and choreography of divisome assembly and cell division are very different from those of *E. coli* (116). In *V. cholerae*, all components of the divisome are located at the new pole at the beginning of the cell cycle and only begin to migrate to the middle of the cell at about 50% of the cell cycle, where they form a loose pre-

607 divisional Z-ring (Fig. 9) (116, 117). The remaining cell division proteins join the early
608 divisome complex in the middle of the cell at about 80% of the cell cycle, and the pre-
609 divisional FtsZ structures fuse into a compact Z-ring (116). The septation process does not
610 begin until about 90% of the cell cycle, leaving a very short time to complete cell division
611 (116). This is puzzling considering the short generation time (18 min.) of *V. cholerae*.

612 In *E. coli*, two systems called Min and nucleoid occlusion (SlmA) work together to allow cell
613 division to occur in the middle of the cell (118, 119). Min directs Z-ring formation to the
614 middle of the cell by inhibiting its formation at the cell poles. SlmA links Z-ring formation to
615 the replication/segregation cycle of the *E. coli* chromosome by preventing its formation over
616 the nucleoid. Min is composed of three proteins: MinC, which blocks Z-ring formation; MinD,
617 which activates MinC; and MinE, which regulates MinCD activity. SlmA binds specifically to
618 DNA and inhibits FtsZ polymerization (120). SlmA binding sites (SBS) are asymmetrically
619 distributed on the *E. coli* chromosome and are mostly absent from ter. This allows cell
620 division to occur only at the very end of the replication/segregation cycle, when the only
621 chromosomal regions remaining in the middle of the cell are the *ter* regions, which lack SBS.
622 *V. cholerae* has orthologs of Min and SlmA. Although MinD shuttles between the poles in *V.*
623 *cholerae*, Min does not appear to be as important as SlmA in the regulation of cell division
624 (117). SBS sites are present on both *V. cholerae* chromosomes except for their *ter*, and their
625 distribution has been shown to be the main driver determining the timing and location of
626 divisome assembly (117). Indeed, the distribution of SBS on Chr1 and Chr2 causes the
627 confinement of FtsZ to the new pole of nascent cells and then contributes to the delay in Z-
628 ring assembly at midcell, after the bulk of Chr1 and Chr2 has replicated and segregated
629 (117).

630 **Organization and segregation of the Ter regions**

631 **Ter organization.** The organization, positioning, and segregation of the chromosome
632 terminus in bacteria, such as *E. coli* or *V. cholerae*, depends on the specific DNA binding

633 protein MatP (121). MatP binds to DNA motifs called *matS*, which are over-represented in
634 the *ter* region and also interacts with components of the divisome (122). Through these
635 interactions, MatP maintains the *ter* region in close proximity to the division site, thereby
636 integrating its segregation into the cell cycle. In *V. cholerae*, both the *ter1* and *ter2* regions
637 have *matS* sites where MatP mediates their spatial confinement (123). However *ter1* and
638 *ter2* behave differently prior to segregation. Sister copies of *ter1* remain together at mid-cell
639 until the end of septation, whereas sister copies of *ter2* segregate before septation is initiated
640 (114, 124). Despite this, sister copies of *ter2* remain in close proximity to the division site and
641 continue to collide with each other during septation (123). When Chr2 completes replication
642 well before Chr1 in a specific mutant strain (where *crtS* was displaced near *ori1*), *ter2*
643 relocates much earlier to the middle of the cell, remains there until Chr1 completes its
644 replication, and segregates at about the same time as *ter1* (15). This suggests that
645 colocalization of *ter1* and *ter2* where cell division occurs is important to coordinate proper
646 segregation prior to cell division. When MatP is inactivated, the position of *ter2* sister copies
647 is no longer restricted and the number of collision events is significantly reduced. On the
648 other hand, without MatP, *ter1* is no longer tethered to the new pole in nascent cells and
649 sister chromatids separate earlier in the cell cycle, while remaining near the center of the cell
650 (123).

651 **Ter segregation.** In most bacterial species, circular chromosomes can form dimers by
652 homologous recombination between sister chromatids, which can compromise chromosome
653 segregation. These dimers are therefore resolved into monomers by adding a crossover at a
654 specific site in the *ter* region, called *dif*, using tyrosine recombinases (XerC and XerD). FtsK,
655 a septal protein, plays two roles in this process: it pumps DNA between daughter cell
656 compartments after divisome assembly but before final septation and activates Xer
657 recombination by interacting directly with XerD. Polar DNA motifs called KOPS direct the
658 loading of FtsK onto the DNA and direct the direction of translocation by pointing from the
659 origin of replication to the *dif* site. It was found in *V. cholerae* that KOPS are overrepresented

and polarized on both Chr1 and Chr2 and that the Chr1 dimer resolution machinery, XerC/XerD/FtsK, also tightly regulates the resolution of Chr2 dimers, even though their resolution sites, *dif1* and *dif2*, are divergent (125). In *E. coli*, FtsK also contributes to the segregation of sister chromosomes in monomeric form under slow growth conditions but is primarily involved in the resolution of chromosome dimers under fast growth conditions (126). In *V. cholerae*, FtsK is involved in the segregation of monomeric sister copies of Chr1 under slow and fast growth conditions due to the prolonged presence of *ter1* sister copies in the middle of the cell (126).

Origin segregation

Ori partition systems. Partitioning complexes contribute to the positioning and segregation of *ori* regions. *V. cholerae* has two distinct ParAB-*parS* systems called ParAB1-*parS1* and ParAB2-*parS2* controlling the localization and partition of *ori1* and *ori2*, respectively (113). ParB1 binds specifically and exclusively to three *parS1* sites proximal to *ori1* (127) and contribute to *ori1* polar positioning (128). A transmembrane protein called HubP acts as a polar organizing factor in *V. cholerae*. HubP interacts directly with ParA1, which in turn directs the ParB1-*parS1* partition complex. As the cell cycle progresses, HubP accumulates at the new pole, followed shortly by ParB1 and then the newly replicated copy of *ori1* (Fig. 9). In the absence of HubP, the pole anchoring of *ori1* is lost, however the partitioning activity of ParAB1 is retained (129). Disruption of ParAB1 leads to *ori1* delocalization from the poles, but this does not seem to affect the segregation of Chr1. It is possible that ParAB1, as in other bacteria, has redundant roles with other players in chromosome segregation, such as cohesins (for example, MukBEF) (128). The polar positioning of *ori1* may also promote the correct sublocalization of certain proteins in the polar region. For example, the ParAB1 system could play a role in launching cell division by driving one of the two SlmA-bound *ori1* regions to the new pole, thereby moving FtsZ to the middle of the cell and triggering septum assembly at the future division site (117, 129).

686 Unlike ParAB1, the ParAB2 segregation system of Chr2 is essential (130). In its absence,
687 segregation problems result in cells without Chr2 that will undergo genomic DNA degradation
688 and eventually stop dividing and die (130, 131). In plasmids, partitioning systems allow them
689 to reside in the nucleoid space where they can interact with the chromosome, rather than at
690 the cell periphery (132, 133). The ParAB2-*parS2* system could also be involved in guiding
691 Chr2 to the nucleoid space.

692 **Interplay between Chromosome Partition and Replication Control.** ParAB proteins are
693 also involved in replication initiation on both chromosomes. Deletion of *parB1* leads to over-
694 initiation of Chr1, and this effect depends on the presence of the *parA1* gene. The exact
695 mechanism by which ParA1 stimulates *ori1* initiation remains unclear, but it appears to
696 involve a direct interaction with DnaA (134). A similar interaction between Soj (ParA ortholog)
697 and DnaA has been reported in *Bacillus subtilis*, where it promotes initiation (135). On the
698 other hand, in the case of Chr2, an indirect positive regulation takes place, as RctB does not
699 interact with ParA2/B2. Instead, regulation occurs through competition for access to DNA
700 binding sites. ParB2 binds to a *parS* site located upstream of the *parA2* gene, spreading
701 locally and partially overlapping with a 39m site (see (136) for review). Additionally, ParB2
702 directly binds to the 5' part of another 39m site, which contains a half *parS2* site. Both ParB2
703 and RctB compete for the binding on this site. As 39m sites are negative regulators of
704 replication, ParB2 here participates in *ori2* activation (85, 137, 138).
705

706 **Intra-chromosomal organization**

707 Using 3C, the conformation of both chromosomes was captured and found to be different
708 (15). While Chr1 adopts an open structure with little interaction of the two replichores, the
709 replichores of Chr2 are more intertwined and often interact suggesting that structural factors
710 may act differently on the two chromosomes (Fig. 9) (15). Such intra-chromosomal
711 interactions, similar to Chr2, have been observed in *Bacillus subtilis* and *Caulobacter*

712 *crescentus* and reflect the bridging of the left and right replichores by SMC condensins (139-
713 141). SMC condensins are recruited to *parS* sites near replication origins and then glide
714 along the replichores tethering them together (140, 141). Given that *V. cholerae* has
715 chromosome-specific ParAB-*parS* machineries, a structural factor may be specifically
716 recruited to one of the chromosomes, a hypothesis that would need more investigation. In *V.*
717 *cholerae*, MukBEF-like condensins, similar to that of *E. coli*, are found. While their function is
718 critical in *E. coli* for chromosome positioning and segregation, deletion of *mukBEF* in *V.*
719 *cholerae* confers no loss of viability and does not alter the positioning and segregation of
720 Chr1 markers including *ori1* (114).

721 **Inter-chromosome interactions**

722 The 3C-derived contact maps reveal *trans* contacts between the two chromosomes. Chr2
723 replichores have a high frequency of contacts with the lower third of Chr1. These contacts
724 start at the chromosome termini (*ter1* and *ter2*) and extend along the chromosomes up to
725 *ori2* for Chr2 and halfway for Chr1 between *ori1* and *ter1* (15). These contacts are not
726 observed in stationary phase, implying that they arise from the replication process. The
727 strong interactions at the termini probably result from the proximity of *ter1* and *ter2* at the
728 division site (mediated by MatP) and their common processing by the segregation
729 machineries (125, 126). Additionally, *ori2* on Chr2 exhibits a strong preference for interacting
730 with the right replichore of Chr1. These interactions start at *crtS* and strengthen downstream,
731 with a focus on a specific region on the left side of *ori2*, near the *parS2* partition sites. This
732 suggests a potential functional interaction that facilitates the action of *crtS* on *ori2* (Fig. 9)
733 (15).

734 **REFLEXION ON DOMESTICATION OF CHR2**

735 *V. cholerae* Chr2 is an example of a well-established and conserved secondary chromosome
736 that has been extensively studied. The evolution of plasmids to megaplasmids and
737 secondary chromosomes has been widely discussed in the literature, mainly with regard to

738 changes in genetic content (accumulation of accessory genes in megaplasmids and
739 acquisition of core genes by secondary chromosomes), nucleotide composition
740 (convergence of overall %GC and codon usage during the long coevolution of chromosomal
741 and extra-chromosomal replicons) and mobility (plasmids and megaplasmids are often
742 conjugative or mobilizable, while secondary chromosomes are usually not) (8, 9, 24). The
743 extensive knowledge of Chr2 presented in this review allows us to look at plasmid
744 domestication from a different perspective - the evolution of maintenance systems to better
745 suit the cell cycle, that ensure stable maintenance of large replicons with low copy numbers
746 in the cell. Compared to other megaplasmids or secondary chromosomes, *V. cholerae* Chr2
747 is the best-studied replicon in this regard.

748 On the one hand, the Chr2 replication system shares similarities with iteron plasmids, but at
749 the same time its maintenance has undergone a number of adaptations. Some of them, such
750 as methylation sites in its iterons or *crtS*-based activation of RctB (81, 85, 142), allow Chr2 to
751 respond well to the cell cycle and fire its replication at the right time. Others enable the
752 proper Chr2 segregation and its specific spatial organization in the cell. These are the
753 *parAB2*-dependent *ori2* partition and the segregation of Chr2 in the closing divisional septum,
754 by hijacking the host systems originally dedicated for the main chromosome (which is
755 achieved by the presence and specific organization of such motifs like KOPS or *dif* in the
756 Chr2 sequence (143)).

757 The presence of all these features, which could not have been acquired simultaneously by
758 the Chr2 ancestor, raises the question of the chronology of evolutionary events during the
759 domestication of Chr2. The sequence of these events can be proposed on the basis of
760 observations of different evolutionary forms on the plasmid-megaplasmid-secondary
761 chromosome continuum in other bacteria, with a particular focus on plasmids carrying
762 replication systems related to *V. cholerae* Chr2.

Only two examples of replicons carrying RctB-like replication initiators have been described in the literature : megaplasmid pA1066 from *V. nigripulchritudo* (144) and Chr2 from *Plesiomonas shigelloides* (145). In terms of their size, which is 250 kb and 300 kb, respectively, they could be expected to be much more plasmid-like than *V. cholerae* Chr2. These replicons exhibit features that may suggest adaptations at various stages in the evolutionary trajectory of Chr2. For instance, their iterons contain methylation sites, which could indicate an early and common adaptation among RctB-type replicons. Additionally, both replicons carry *parAB* partition genes located close to their origin of replication (144, 145), as typically observed in replicons larger than 25 kb (133). It is worth noting that pA1066 carries a putative conjugation system and is non-essential (144) while most plasmids larger than 250 kb are non-mobilizable (146), suggesting the loss of mobility and acquisition of housekeeping genes as potential late evolutionary events. Interestingly, despite its relatively small size, *P. shigelloides* already demonstrates the appropriate organization of the KOPS motif and putative *dif* site, suggesting the early utilization of FtsK and XerCD mechanisms in the division partition (145). This finding indicates that such adaptations can occur relatively early in the plasmid domestication process. In *P. shigelloides* Chr1, no *crtS*-like sequence was identified, and no synchronization of termination between Chr1 and Chr2 was observed in the *P. shigelloides* strain (145). These observations suggest that the *crtS* mechanism may have appeared later in the evolution of *V. cholerae* Chr2. Furthermore, the RctB proteins of both pA1066 and *P. shigelloides* Chr2 find a nearly complete structural match to RctB from *V. cholerae* Chr2, spanning all four domains. This suggests that the appearance of domains I and IV likely occurred early in the evolution of RctB. To gain a deeper understanding of the evolutionary process of plasmids transitioning into secondary chromosomes, it is imperative to conduct further analysis on the replication of these replicons, as well as other replicons carrying replication systems related to *V. cholerae* Chr2.

PERSPECTIVES

Vibrio is the best-studied model of bacteria with a bipartite genome in terms of DNA replication mechanisms. Despite significant progress in understanding the regulation of Chr2 replication, there are still many details that remain unknown. Current research aims to unravel the full picture of *ori2* regulation. These studies include such questions as how the passage of replication forks through the *crtS* site is sensed and the role of Lrp in this process, how *crtS* alters RctB activity, and how activated RctB affects inactive *ori2*. Still unresolved is the mechanism of intramolecular handcuffing in *ori2*, dependent on 39m and 29m, and the complete structure of the RctB protein, in particular the domain IV, which is involved in this process.

The limited number of described plasmids and megaplasmids with replication initiators related to RctB has hindered our full understanding of the evolutionary processes involved in establishing a multipartite genome. However, recent exploration of databases has now facilitated the identification of RctB relatives not only in *Vibrio* but also in strains from Enterobacterales (145). Conducting comparative genomics and functional studies on plasmids containing these initiator genes should provide valuable insights into these evolutionary questions.

Finally, similar analyses should be extended to other important bacterial models with multipartite genomes, such as *Agrobacterium*, *Brucella*, *Burkholderia*, *Leptospira*, *Sinorhizobium* or *Rhodobacter*. It should be remembered that the secondary replicons in each of these groups of bacteria arose independently, from plasmids carrying different replication systems and in different genetic contexts. Therefore, the mechanisms that govern their replication and maintenance may be quite different to those described for *Vibrio*.

ACKNOWLEDGMENTS

Our lab is funded by the Institut Pasteur, the Institut National de la Santé et de la Recherche Médicale (INSERM) and the Centre National de la Recherche Scientifique (CNRS). This work was supported by the French National Research Agency, Jeunes Chercheurs [ANR-19-CE12-0001] and Laboratoires d'Excellence [ANR-10-LABX-62-IBEID]. This work was supported by the Fondation pour la Recherche Médicale, Equipe FRM EQU202103012569, and FDM202106013531 to LAMBERIOUX Morgan. The authors have no conflict of interest to declare.

REFERENCES

1. Frage B, Dohlemann J, Robledo M, Lucena D, Sobetzko P, Graumann PL, Becker A. 2016. Spatiotemporal choreography of chromosome and megaplasmids in the Sinorhizobium meliloti cell cycle. Mol Microbiol 100:808-23.
2. Deghelt M, Mullier C, Sternon JF, Francis N, Laloux G, Dotreppe D, Van der Henst C, Jacobs-Wagner C, Letesson JJ, De Bolle X. 2014. G1-arrested newborn cells are the predominant infectious form of the pathogen Brucella abortus. Nat Commun 5:4366.
3. Dubarry N, Willis CR, Ball G, Lesterlin C, Armitage JP. 2019. In Vivo Imaging of the Segregation of the 2 Chromosomes and the Cell Division Proteins of Rhodobacter sphaeroides Reveals an Unexpected Role for MipZ. MBio 10.
4. Du WL, Dubarry N, Passot FM, Kamgoue A, Murray H, Lane D, Pasta F. 2016. Orderly Replication and Segregation of the Four Replicons of Burkholderia cenocepacia J2315. PLoS Genet 12:e1006172.
5. Xie BB, Rong JC, Tang BL, Wang S, Liu G, Qin QL, Zhang XY, Zhang W, She Q, Chen Y, Li F, Li S, Chen XL, Luo H, Zhang YZ. 2021. Evolutionary Trajectory of the Replication Mode of Bacterial Replicons. mBio 12.
6. Ren Z, Liao Q, Karaboja X, Barton IS, Schantz EG, Mejia-Santana A, Fuqua C, Wang X. 2022. Conformation and dynamic interactions of the multipartite genome in Agrobacterium tumefaciens. Proc Natl Acad Sci U S A 119.
7. Rasmussen T, Jensen RB, Skovgaard O. 2007. The two chromosomes of Vibrio cholerae are initiated at different time points in the cell cycle. EMBO J 26:3124-31.
8. Harrison PW, Lower RP, Kim NK, Young JP. 2010. Introducing the bacterial 'chromid': not a chromosome, not a plasmid. Trends Microbiol 18:141-8.
9. diCenzo GC, Finan TM. 2017. The Divided Bacterial Genome: Structure, Function, and Evolution. Microbiol Mol Biol Rev 81.
10. Reen FJ, Almagro-Moreno S, Ussery D, Boyd EF. 2006. The genomic code: inferring Vibrionaceae niche specialization. Nat Rev Microbiol 4:697-704.
11. diCenzo GC, Mengoni A, Perrin E. 2019. Chromids Aid Genome Expansion and Functional Diversification in the Family Burkholderiaceae. Mol Biol Evol 36:562-574.
12. Xie G, Johnson SL, Davenport KW, Rajavel M, Waldminghaus T, Detter JC, Chain PS, Sozhamannan S. 2017. Exception to the Rule: Genomic Characterization of Naturally Occurring Unusual Vibrio cholerae Strains with a Single Chromosome. Int J Genomics 2017:8724304.
13. Bruhn M, Schindler D, Kemter FS, Wiley MR, Chase K, Koroleva GI, Palacios G, Sozhamannan S, Waldminghaus T. 2018. Functionality of Two Origins of Replication in Vibrio cholerae Strains With a Single Chromosome. Front Microbiol 9:2932.
14. Yamamoto S, Lee KI, Morita M, Arakawa E, Izumiya H, Ohnishi M. 2018. Single Circular Chromosome Identified from the Genome Sequence of the Vibrio cholerae O1 bv. El Tor Ogawa Strain V060002. Genome Announc 6.
15. Val ME, Marbouty M, de Lemos Martins F, Kennedy SP, Kemble H, Bland MJ, Possoz C, Koszul R, Skovgaard O, Mazel D. 2016. A checkpoint control orchestrates the replication of the two chromosomes of Vibrio cholerae. Sci Adv 2:e1501914.
16. Guo X, Flores M, Mavingui P, Fuentes SI, Hernandez G, Davila G, Palacios R. 2003. Natural genomic design in Sinorhizobium meliloti: novel genomic architectures. Genome Res 13:1810-7.
17. Liao Q, Ren Z, Wiesler EE, Fuqua C, Wang X. 2022. A dicentric bacterial chromosome requires XerC/D site-specific recombinases for resolution. Curr Biol 32:3609-3618 e7.
18. Mori JF, Kanaly RA. 2022. Natural Chromosome-Chromid Fusion across rRNA Operons in a Burkholderiaceae Bacterium. Microbiol Spectr doi:10.1128/spectrum.02225-21:e0222521.

19. Sonnenberg CB, Kahlke T, Haugen P. 2020. Vibrionaceae core, shell and cloud genes are non-randomly distributed on Chr 1: An hypothesis that links the genomic location of genes with their intracellular placement. BMC Genomics 21:695.
20. Couturier E, Rocha EP. 2006. Replication-associated gene dosage effects shape the genomes of fast-growing bacteria but only for transcription and translation genes. Mol Microbiol 59:1506-18.
21. Soler-Bistue A, Mondotte JA, Bland MJ, Val ME, Saleh MC, Mazel D. 2015. Genomic location of the major ribosomal protein gene locus determines Vibrio cholerae global growth and infectivity. PLoS Genet 11:e1005156.
22. Soler-Bistue A, Timmermans M, Mazel D. 2017. The Proximity of Ribosomal Protein Genes to oriC Enhances Vibrio cholerae Fitness in the Absence of Multifork Replication. MBio 8.
23. Soler-Bistue A, Aguilar-Pierle S, Garcia-Garcera M, Val ME, Sismeiro O, Varet H, Sieira R, Krin E, Skovgaard O, Comerci DJ, Rocha EPC, Mazel D. 2020. Macromolecular crowding links ribosomal protein gene dosage to growth rate in Vibrio cholerae. BMC Biol 18:43.
24. Hall JPJ, Botelho J, Cazares A, Baltrus DA. 2022. What makes a megaplasmid? Philos Trans R Soc Lond B Biol Sci 377:20200472.
25. Jaskolska M, Adams DW, Blokesch M. 2022. Two defence systems eliminate plasmids from seventh pandemic Vibrio cholerae. Nature doi:10.1038/s41586-022-04546-y.
26. Heidelberg JF, Eisen JA, Nelson WC, Clayton RA, Gwinn ML, Dodson RJ, Haft DH, Hickey EK, Peterson JD, Umayam L, Gill SR, Nelson KE, Read TD, Tettelin H, Richardson D, Ermolaeva MD, Vamathevan J, Bass S, Qin H, Dragoi I, Sellers P, McDonald L, Utterback T, Fleishmann RD, Nierman WC, White O, Salzberg SL, Smith HO, Colwell RR, Mekalanos JJ, Venter JC, Fraser CM. 2000. DNA sequence of both chromosomes of the cholera pathogen Vibrio cholerae. Nature 406:477-83.
27. Duigou S, Knudsen KG, Skovgaard O, Egan ES, Lobner-Olesen A, Waldor MK. 2006. Independent control of replication initiation of the two Vibrio cholerae chromosomes by DnaA and RctB. J Bacteriol 188:6419-24.
28. Egan ES, Waldor MK. 2003. Distinct replication requirements for the two Vibrio cholerae chromosomes. Cell 114:521-30.
29. Demarre G, Chattoraj DK. 2010. DNA adenine methylation is required to replicate both Vibrio cholerae chromosomes once per cell cycle. PLoS Genet 6:e1000939.
30. Koch B, Ma X, Lobner-Olesen A. 2010. Replication of Vibrio cholerae chromosome I in Escherichia coli: dependence on dam methylation. J Bacteriol 192:3903-14.
31. Katayama T, Kasho K, Kawakami H. 2017. The DnaA Cycle in Escherichia coli: Activation, Function and Inactivation of the Initiator Protein. Front Microbiol 8:2496.
32. Berger M, Wolde PRT. 2022. Robust replication initiation from coupled homeostatic mechanisms. Nat Commun 13:6556.
33. Marinus MG, Lobner-Olesen A. 2014. DNA Methylation. EcoSal Plus 6.
34. von Freiesleben U, Krekling MA, Hansen FG, Lobner-Olesen A. 2000. The eclipse period of Escherichia coli. EMBO J 19:6240-8.
35. Katayama T, Ozaki S, Keyamura K, Fujimitsu K. 2010. Regulation of the replication cycle: conserved and diverse regulatory systems for DnaA and oriC. Nat Rev Microbiol 8:163-70.
36. Kasho K, Katayama T. 2013. DnaA binding locus datA promotes DnaA-ATP hydrolysis to enable cell cycle-coordinated replication initiation. Proc Natl Acad Sci U S A 110:936-41.
37. Frimodt-Moller J, Charbon G, Krogfelt KA, Lobner-Olesen A. 2016. DNA Replication Control Is Linked to Genomic Positioning of Control Regions in Escherichia coli. PLoS Genet 12:e1006286.
38. Fujimitsu K, Senriuchi T, Katayama T. 2009. Specific genomic sequences of E. coli promote replicational initiation by directly reactivating ADP-DnaA. Genes Dev 23:1221-33.
39. Keyamura K, Fujikawa N, Ishida T, Ozaki S, Su'etsugu M, Fujimitsu K, Kagawa W, Yokoyama S, Kurumizaka H, Katayama T. 2007. The interaction of DiaA and DnaA regulates the replication

cycle in E. coli by directly promoting ATP DnaA-specific initiation complexes. Genes Dev 21:2083-99.
40. Ishida T, Akimitsu N, Kashioka T, Hatano M, Kubota T, Ogata Y, Sekimizu K, Katayama T. 2004. DiaA, a novel DnaA-binding protein, ensures the timely initiation of Escherichia coli chromosome replication. J Biol Chem 279:45546-55.
41. Gross MH, Konieczny I. 2020. Polyphosphate induces the proteolysis of ADP-bound fraction of initiator to inhibit DNA replication initiation upon stress in Escherichia coli. Nucleic Acids Res doi:10.1093/nar/gkaa217.
42. Kemter FS, Messerschmidt SJ, Schallopp N, Sobetzko P, Lang E, Bunk B, Sproer C, Teschler JK, Yildiz FH, Overmann J, Waldminghaus T. 2018. Synchronous termination of replication of the two chromosomes is an evolutionary selected feature in Vibrionaceae. PLoS Genet 14:e1007251.
43. Ferullo DJ, Cooper DL, Moore HR, Lovett ST. 2009. Cell cycle synchronization of Escherichia coli using the stringent response, with fluorescence labeling assays for DNA content and replication. Methods 48:8-13.
44. Kemter FS, Schallopp N, Sperlea T, Serrania J, Sobetzko P, Fritz G, Waldminghaus T. 2019. Stringent response leads to continued cell division and a temporal restart of DNA replication after initial shutdown in Vibrio cholerae. Mol Microbiol 111:1617-1637.
45. Kim JW, Bugata V, Cortes-Cortes G, Quevedo-Martinez G, Camps M. 2020. Mechanisms of Theta Plasmid Replication in Enterobacteria and Implications for Adaptation to Its Host. EcoSal Plus 9.
46. Konieczny I, Bury K, Wawrzycka A, Wegrzyn K. 2014. Iteron Plasmids. Microbiol Spectr 2.
47. Filutowicz M, Davis G, Greener A, Helinski DR. 1985. Autorepressor properties of the pi-initiation protein encoded by plasmid R6K. Nucleic Acids Res 13:103-14.
48. Vocke C, Bastia D. 1985. The replication initiator protein of plasmid pSC101 is a transcriptional repressor of its own cistron. Proc Natl Acad Sci U S A 82:2252-6.
49. Venkova-Canova T, Chattoraj DK. 2011. Transition from a plasmid to a chromosomal mode of replication entails additional regulators. Proc Natl Acad Sci U S A 108:6199-204.
50. Venkova-Canova T, Saha A, Chattoraj DK. 2012. A 29-mer site regulates transcription of the initiator gene as well as function of the replication origin of Vibrio cholerae chromosome II. Plasmid 67:102-10.
51. Fournes F, Niault T, Czarnecki J, Tissier-Visconti A, Mazel D, Val ME. 2021. The coordinated replication of Vibrio cholerae's two chromosomes required the acquisition of a unique domain by the RctB initiator. Nucleic Acids Res 49:11119-11133.
52. Orlova N, Gerding M, Ivashkiv O, Olinares PDB, Chait BT, Waldor MK, Jeruzalmi D. 2017. The replication initiator of the cholera pathogen's second chromosome shows structural similarity to plasmid initiators. Nucleic Acids Res 45:3724-3737.
53. Jha JK, Demarre G, Venkova-Canova T, Chattoraj DK. 2012. Replication regulation of Vibrio cholerae chromosome II involves initiator binding to the origin both as monomer and as dimer. Nucleic Acids Res 40:6026-38.
54. Wickner S, Skowyra D, Hoskins J, McKenney K. 1992. DnaJ, DnaK, and GrpE heat shock proteins are required in oriP1 DNA replication solely at the RepA monomerization step. Proc Natl Acad Sci U S A 89:10345-9.
55. Jha JK, Li M, Ghirlando R, Miller Jenkins LM, Wlodawer A, Chattoraj D. 2017. The DnaK Chaperone Uses Different Mechanisms To Promote and Inhibit Replication of Vibrio cholerae Chromosome 2. MBio 8.
56. Diaz-Lopez T, Lages-Gonzalo M, Serrano-Lopez A, Alfonso C, Rivas G, Diaz-Orejas R, Giraldo R. 2003. Structural changes in RepA, a plasmid replication initiator, upon binding to origin DNA. J Biol Chem 278:18606-16.
57. Wegrzyn K, Zabrocka E, Bury K, Tomiczek B, Wieczor M, Czub J, Uciechowska U, Moreno-Del Alamo M, Walkow U, Grochowina I, Dutkiewicz R, Bujnicki JM, Giraldo R, Konieczny I. 2021.

Defining a novel domain that provides an essential contribution to site-specific interaction of Rep protein with DNA. Nucleic Acids Res 49:3394-3408.
58. Jha JK, Ghirlando R, Chattoraj DK. 2014. Initiator protein dimerization plays a key role in replication control of Vibrio cholerae chromosome 2. Nucleic Acids Res 42:10538-49.
59. Gerding MA, Chao MC, Davis BM, Waldor MK. 2015. Molecular Dissection of the Essential Features of the Origin of Replication of the Second Vibrio cholerae Chromosome. MBio 6:e00973.
60. Chatterjee S, Jha JK, Ciaccia P, Venkova T, Chattoraj DK. 2020. Interactions of replication initiator RctB with single- and double-stranded DNA in origin opening of Vibrio cholerae chromosome 2. Nucleic Acids Res doi:10.1093/nar/gkaa826.
61. Ozaki S, Katayama T. 2012. Highly organized DnaA-oriC complexes recruit the single-stranded DNA for replication initiation. Nucleic Acids Res 40:1648-65.
62. Sakiyama Y, Kasho K, Noguchi Y, Kawakami H, Katayama T. 2017. Regulatory dynamics in the ternary DnaA complex for initiation of chromosomal replication in Escherichia coli. Nucleic Acids Res 45:12354-12373.
63. Duderstadt KE, Chuang K, Berger JM. 2011. DNA stretching by bacterial initiators promotes replication origin opening. Nature 478:209-13.
64. Ozaki S, Kawakami H, Nakamura K, Fujikawa N, Kagawa W, Park SY, Yokoyama S, Kurumizaka H, Katayama T. 2008. A common mechanism for the ATP-DnaA-dependent formation of open complexes at the replication origin. J Biol Chem 283:8351-62.
65. Ramachandran R, Jha J, Paulsson J, Chattoraj D. 2017. Random versus Cell Cycle-Regulated Replication Initiation in Bacteria: Insights from Studying Vibrio cholerae Chromosome 2. Microbiol Mol Biol Rev 81.
66. Das N, Valjavec-Gratian M, Basuray AN, Fekete RA, Papp PP, Paulsson J, Chattoraj DK. 2005. Multiple homeostatic mechanisms in the control of P1 plasmid replication. Proc Natl Acad Sci U S A 102:2856-61.
67. Chattoraj DK. 2000. Control of plasmid DNA replication by iterons: no longer paradoxical. Mol Microbiol 37:467-76.
68. Komori H, Matsunaga F, Higuchi Y, Ishiai M, Wada C, Miki K. 1999. Crystal structure of a prokaryotic replication initiator protein bound to DNA at 2.6 A resolution. EMBO J 18:4597-607.
69. Ingmer H, Fong EL, Cohen SN. 1995. Monomer-dimer equilibrium of the pSC101 RepA protein. J Mol Biol 250:309-14.
70. Giraldo R, Fernandez-Tornero C, Evans PR, Diaz-Orejas R, Romero A. 2003. A conformational switch between transcriptional repression and replication initiation in the RepA dimerization domain. Nat Struct Biol 10:565-71.
71. Wickner S, Hoskins J, McKenney K. 1991. Monomerization of RepA dimers by heat shock proteins activates binding to DNA replication origin. Proc Natl Acad Sci U S A 88:7903-7.
72. Dibbens JA, Muraiso K, Chattoraj DK. 1997. Chaperone-mediated reduction of RepA dimerization is associated with RepA conformational change. Mol Microbiol 26:185-95.
73. McEachern MJ, Bott MA, Tooker PA, Helinski DR. 1989. Negative control of plasmid R6K replication: possible role of intermolecular coupling of replication origins. Proc Natl Acad Sci U S A 86:7942-6.
74. Chattoraj DK, Mason RJ, Wickner SH. 1988. Mini-P1 plasmid replication: the autoregulation-sequestration paradox. Cell 52:551-7.
75. Molina-Garcia L, Gasset-Rosa F, Moreno-Del Alamo M, Fernandez-Tresguerres ME, Moreno-Diaz de la Espina S, Lurz R, Giraldo R. 2016. Functional amyloids as inhibitors of plasmid DNA replication. Sci Rep 6:25425.
76. Zzaman S, Bastia D. 2005. Oligomeric initiator protein-mediated DNA looping negatively regulates plasmid replication in vitro by preventing origin melting. Mol Cell 20:833-43.

77. Uga H, Matsunaga F, Wada C. 1999. Regulation of DNA replication by iterons: an interaction between the ori2 and incC regions mediated by RepE-bound iterons inhibits DNA replication of mini-F plasmid in Escherichia coli. EMBO J 18:3856-67.
78. Brendler T, Abeles A, Austin S. 1995. A protein that binds to the P1 origin core and the oriC 13mer region in a methylation-specific fashion is the product of the host seqA gene. EMBO J 14:4083-9.
79. Brendler T, Abeles A, Austin S. 1991. Critical sequences in the core of the P1 plasmid replication origin. J Bacteriol 173:3935-42.
80. Abeles AL, Austin SJ. 1987. P1 plasmid replication requires methylated DNA. EMBO J 6:3185-9.
81. Val ME, Kennedy SP, Soler-Bistue AJ, Barbe V, Bouchier C, Ducos-Galand M, Skovgaard O, Mazel D. 2014. Fuse or die: how to survive the loss of Dam in Vibrio cholerae. Mol Microbiol 91:665-78.
82. Baek JH, Chattoraj DK. 2014. Chromosome I controls chromosome II replication in Vibrio cholerae. PLoS Genet 10:e1004184.
83. Egan ES, Lobner-Olesen A, Waldor MK. 2004. Synchronous replication initiation of the two Vibrio cholerae chromosomes. Curr Biol 14:R501-2.
84. Stokke C, Waldminghaus T, Skarstad K. 2011. Replication patterns and organization of replication forks in Vibrio cholerae. Microbiology (Reading) 157:695-708.
85. de Lemos Martins F, Fournes F, Mazzuoli MV, Mazel D, Val ME. 2018. Vibrio cholerae chromosome 2 copy number is controlled by the methylation-independent binding of its monomeric initiator to the chromosome 1 crtS site. Nucleic Acids Res 46:10145-10156.
86. Sanchez-Romero MA, Casadesus J. 2020. The bacterial epigenome. Nat Rev Microbiol 18:7-20.
87. Postow L, Crisona NJ, Peter BJ, Hardy CD, Cozzarelli NR. 2001. Topological challenges to DNA replication: conformations at the fork. Proc Natl Acad Sci U S A 98:8219-26.
88. Arias-Cartin R, Dobihal GS, Campos M, Surovtsev IV, Parry B, Jacobs-Wagner C. 2017. Replication fork passage drives asymmetric dynamics of a critical nucleoid-associated protein in Caulobacter. EMBO J 36:301-318.
89. Loot C, Bikard D, Rachlin A, Mazel D. 2010. Cellular pathways controlling integron cassette site folding. EMBO J 29:2623-34.
90. Ramachandran R, Ciaccia PN, Filsuf TA, Jha JK, Chattoraj DK. 2018. Chromosome 1 licenses chromosome 2 replication in Vibrio cholerae by doubling the crtS gene dosage. PLoS Genet 14:e1007426.
91. Ciaccia PN, Ramachandran R, Chattoraj DK. 2018. A Requirement for Global Transcription Factor Lrp in Licensing Replication of Vibrio cholerae Chromosome 2. Front Microbiol 9:2103.
92. Cui Y, Wang Q, Stormo GD, Calvo JM. 1995. A consensus sequence for binding of Lrp to DNA. J Bacteriol 177:4872-80.
93. Beloin C, Jeusset J, Revet B, Mirambeau G, Le Hegarat F, Le Cam E. 2003. Contribution of DNA conformation and topology in right-handed DNA wrapping by the Bacillus subtilis LrpC protein. J Biol Chem 278:5333-42.
94. Kasho K, Fujimitsu K, Matoba T, Oshima T, Katayama T. 2014. Timely binding of IHF and Fis to DARS2 regulates ATP-DnaA production and replication initiation. Nucleic Acids Res 42:13134-49.
95. Miyoshi K, Tatsumoto Y, Ozaki S, Katayama T. 2021. Negative feedback for DARS2-Fis complex by ATP-DnaA supports the cell cycle-coordinated regulation for chromosome replication. Nucleic Acids Res 49:12820-12835.
96. Zamora M, Ziegler CA, Freddolino PL, Wolfe AJ. 2020. A Thermosensitive, Phase-Variable Epigenetic Switch: pap Revisited. Microbiol Mol Biol Rev 84.
97. Kothapalli R, Ghirlando R, Khan ZA, Chatterjee S, Kedei N, Chattoraj DK. 2022. The dimerization interface of initiator RctB governs chaperone and enhancer dependence of Vibrio cholerae chromosome 2 replication. Nucleic Acids Res doi:10.1093/nar/gkac210.

98. Wegrzyn KE, Gross M, Uciechowska U, Konieczny I. 2016. Replisome Assembly at Bacterial Chromosomes and Iteron Plasmids. Front Mol Biosci 3:39.
99. Baker KS, Dallman TJ, Field N, Childs T, Mitchell H, Day M, Weill FX, Lefevre S, Tourdjman M, Hughes G, Jenkins C, Thomson N. 2018. Horizontal antimicrobial resistance transfer drives epidemics of multiple Shigella species. Nat Commun 9:1462.
100. Arias-Palomo E, O'Shea VL, Hood IV, Berger JM. 2013. The bacterial DnaC helicase loader is a DnaB ring breaker. Cell 153:438-48.
101. Smits WK, Goranov AI, Grossman AD. 2010. Ordered association of helicase loader proteins with the Bacillus subtilis origin of replication in vivo. Mol Microbiol 75:452-61.
102. Brezellec P, Vallet-Gely I, Possoz C, Quevillon-Cheruel S, Ferat JL. 2016. DciA is an ancestral replicative helicase operator essential for bacterial replication initiation. Nat Commun 7:13271.
103. Marsin S, Adam Y, Cargemel C, Andreani J, Baconnais S, Legrand P, Li de la Sierra-Gallay I, Humbert A, Aumont-Nicaise M, Velours C, Ochsenbein F, Durand D, Le Cam E, Walbott H, Possoz C, Quevillon-Cheruel S, Ferat JL. 2021. Study of the DnaB:DciA interplay reveals insights into the primary mode of loading of the bacterial replicative helicase. Nucleic Acids Res 49:6569-6586.
104. Cargemel C, Walbott H, Durand D, Legrand P, Ouldali M, Ferat JL, Marsin S, Quevillon-Cheruel S. 2022. The apo-form of the Vibrio cholerae replicative helicase DnaB is a labile and inactive planar trimer of dimers. FEBS Lett 596:2031-2040.
105. Datta HJ, Khatri GS, Bastia D. 1999. Mechanism of recruitment of DnaB helicase to the replication origin of the plasmid pSC101. Proc Natl Acad Sci U S A 96:73-8.
106. Jiang Y, Pacek M, Helinski DR, Konieczny I, Toukdarian A. 2003. A multifunctional plasmid-encoded replication initiation protein both recruits and positions an active helicase at the replication origin. Proc Natl Acad Sci U S A 100:8692-7.
107. Caspi R, Pacek M, Consiglieri G, Helinski DR, Toukdarian A, Konieczny I. 2001. A broad host range replicon with different requirements for replication initiation in three bacterial species. EMBO J 20:3262-71.
108. Bartlett TM, Bratton BP, Duvshani A, Miguel A, Sheng Y, Martin NR, Nguyen JP, Persat A, Desmarais SM, VanNieuwenhze MS, Huang KC, Zhu J, Shaevitz JW, Gitai Z. 2017. A Periplasmic Polymer Curves Vibrio cholerae and Promotes Pathogenesis. Cell 168:172-185 e15.
109. Espinosa E, Paly E, Barre FX. 2020. High-Resolution Whole-Genome Analysis of Sister-Chromatid Contacts. Mol Cell 79:857-869 e3.
110. Duggin IG, Wake RG, Bell SD, Hill TM. 2008. The replication fork trap and termination of chromosome replication. Mol Microbiol 70:1323-33.
111. Galli E, Ferat JL, Desfontaines JM, Val ME, Skovgaard O, Barre FX, Possoz C. 2019. Replication termination without a replication fork trap. Sci Rep 9:8315.
112. Wang X, Rudner DZ. 2014. Spatial organization of bacterial chromosomes. Curr Opin Microbiol 22:66-72.
113. Fogel MA, Waldor MK. 2005. Distinct segregation dynamics of the two Vibrio cholerae chromosomes. Mol Microbiol 55:125-36.
114. David A, Demarre G, Muresan L, Paly E, Barre FX, Possoz C. 2014. The two Cis-acting sites, parS1 and oriC1, contribute to the longitudinal organisation of Vibrio cholerae chromosome I. PLoS Genet 10:e1004448.
115. Du S, Lutkenhaus J. 2017. Assembly and activation of the Escherichia coli divisome. Mol Microbiol 105:177-187.
116. Galli E, Paly E, Barre FX. 2017. Late assembly of the Vibrio cholerae cell division machinery postpones septation to the last 10% of the cell cycle. Sci Rep 7:44505.
117. Galli E, Poidevin M, Le Bars R, Desfontaines JM, Muresan L, Paly E, Yamaichi Y, Barre FX. 2016. Cell division licensing in the multi-chromosomal Vibrio cholerae bacterium. Nat Microbiol 1:16094.

118. Schumacher MA. 2017. Bacterial Nucleoid Occlusion: Multiple Mechanisms for Preventing Chromosome Bisection During Cell Division. Subcell Biochem 84:267-298.
119. Adams DW, Wu LJ, Errington J. 2014. Cell cycle regulation by the bacterial nucleoid. Curr Opin Microbiol 22:94-101.
120. Cho H, McManus HR, Dove SL, Bernhardt TG. 2011. Nucleoid occlusion factor SlmA is a DNA-activated FtsZ polymerization antagonist. Proc Natl Acad Sci U S A 108:3773-8.
121. Mercier R, Petit MA, Schbath S, Robin S, El Karoui M, Boccard F, Espeli O. 2008. The MatP/matS site-specific system organizes the terminus region of the E. coli chromosome into a macrodomain. Cell 135:475-85.
122. Espeli O, Borne R, Dupaigne P, Thiel A, Gigant E, Mercier R, Boccard F. 2012. A MatP-divisome interaction coordinates chromosome segregation with cell division in E. coli. EMBO J 31:3198-211.
123. Demarre G, Galli E, Muresan L, Paly E, David A, Possoz C, Barre FX. 2014. Differential management of the replication terminus regions of the two Vibrio cholerae chromosomes during cell division. PLoS Genet 10:e1004557.
124. Srivastava P, Fekete RA, Chattoraj DK. 2006. Segregation of the replication terminus of the two Vibrio cholerae chromosomes. J Bacteriol 188:1060-70.
125. Val ME, Kennedy SP, El Karoui M, Bonne L, Chevalier F, Barre FX. 2008. FtsK-dependent dimer resolution on multiple chromosomes in the pathogen Vibrio cholerae. PLoS Genet 4:e1000201.
126. Galli E, Midonet C, Paly E, Barre FX. 2017. Fast growth conditions uncouple the final stages of chromosome segregation and cell division in Escherichia coli. PLoS Genet 13:e1006702.
127. Debaugny RE, Sanchez A, Rech J, Labourdette D, Dorignac J, Geniet F, Palmeri J, Parmeggiani A, Boudsocq F, Anton Leberre V, Walter JC, Bouet JY. 2018. A conserved mechanism drives partition complex assembly on bacterial chromosomes and plasmids. Mol Syst Biol 14:e8516.
128. Fogel MA, Waldor MK. 2006. A dynamic, mitotic-like mechanism for bacterial chromosome segregation. Genes Dev 20:3269-82.
129. Possoz C, Yamaichi Y, Galli E, Ferat JL, Barre FX. 2022. Vibrio cholerae Chromosome Partitioning without Polar Anchoring by HubP. Genes (Basel) 13.
130. Yamaichi Y, Fogel MA, Waldor MK. 2007. par genes and the pathology of chromosome loss in Vibrio cholerae. Proc Natl Acad Sci U S A 104:630-5.
131. Yuan J, Yamaichi Y, Waldor MK. 2011. The three vibrio cholerae chromosome II-encoded ParE toxins degrade chromosome I following loss of chromosome II. J Bacteriol 193:611-9.
132. Le Gall A, Cattoni DI, Guilhas B, Mathieu-Demaziere C, Oudjedi L, Fiche JB, Rech J, Abrahamsson S, Murray H, Bouet JY, Nollmann M. 2016. Bacterial partition complexes segregate within the volume of the nucleoid. Nat Commun 7:12107.
133. Planchenault C, Pons MC, Schiavon C, Siguier P, Rech J, Guynet C, Dauverd-Girault J, Cury J, Rocha EPC, Junier I, Cornet F, Espeli O. 2020. Intracellular Positioning Systems Limit the Entropic Eviction of Secondary Replicons Toward the Nucleoid Edges in Bacterial Cells. J Mol Biol 432:745-761.
134. Kadoya R, Baek JH, Sarker A, Chattoraj DK. 2011. Participation of chromosome segregation protein ParAI of Vibrio cholerae in chromosome replication. J Bacteriol 193:1504-14.
135. Murray H, Errington J. 2008. Dynamic control of the DNA replication initiation protein DnaA by Soj/ParA. Cell 135:74-84.
136. Val ME, Soler-Bistue A, Bland MJ, Mazel D. 2014. Management of multipartite genomes: the Vibrio cholerae model. Curr Opin Microbiol 22:120-6.
137. Yamaichi Y, Gerding MA, Davis BM, Waldor MK. 2011. Regulatory cross-talk links Vibrio cholerae chromosome II replication and segregation. PLoS Genet 7:e1002189.
138. Venkova-Canova T, Baek JH, Fitzgerald PC, Blokesch M, Chattoraj DK. 2013. Evidence for two different regulatory mechanisms linking replication and segregation of vibrio cholerae chromosome II. PLoS Genet 9:e1003579.

139. Le TB, Imakaev MV, Mirny LA, Laub MT. 2013. High-resolution mapping of the spatial organization of a bacterial chromosome. Science 342:731-4.
140. Marbouty M, Le Gall A, Cattoni DI, Cournac A, Koh A, Fiche JB, Mozziconacci J, Murray H, Koszul R, Nollmann M. 2015. Condensin- and Replication-Mediated Bacterial Chromosome Folding and Origin Condensation Revealed by Hi-C and Super-resolution Imaging. Mol Cell 59:588-602.
141. Wang X, Le TB, Lajoie BR, Dekker J, Laub MT, Rudner DZ. 2015. Condensin promotes the juxtaposition of DNA flanking its loading site in Bacillus subtilis. Genes Dev 29:1661-75.
142. Val ME, Skovgaard O, Ducos-Galand M, Bland MJ, Mazel D. 2012. Genome engineering in Vibrio cholerae: a feasible approach to address biological issues. PLoS Genet 8:e1002472.
143. Touzain F, Petit MA, Schbath S, El Karoui M. 2011. DNA motifs that sculpt the bacterial chromosome. Nat Rev Microbiol 9:15-26.
144. Le Roux F, Labreuche Y, Davis BM, Iqbal N, Mangenot S, Goarant C, Mazel D, Waldor MK. 2011. Virulence of an emerging pathogenic lineage of Vibrio nigripulchritudo is dependent on two plasmids. Environ Microbiol 13:296-306.
145. Adam Y, Brezellec P, Espinosa E, Besombes A, Naquin D, Paly E, Possoz C, van Dijk E, Barre FX, Ferat JL. 2022. Plesiomonas shigelloides, an Atypical Enterobacterales with a Vibrio-Related Secondary Chromosome. Genome Biol Evol 14.
146. Smillie C, Garcillan-Barcia MP, Francia MV, Rocha EP, de la Cruz F. 2010. Mobility of plasmids. Microbiol Mol Biol Rev 74:434-52.
147. Jiang C, Tanaka M, Nishikawa S, Mino S, Romalde JL, Thompson FL, Gomez-Gil B, Sawabe T. 2021. Vibrio Clade 3.0: New Vibrionaceae Evolutionary Units Using Genome-Based Approach. Curr Microbiol 79:10.
148. Katoh K, Standley DM. 2013. MAFFT multiple sequence alignment software version 7: improvements in performance and usability. Mol Biol Evol 30:772-80.
149. Minh BQ, Schmidt HA, Chernomor O, Schrempf D, Woodhams MD, von Haeseler A, Lanfear R. 2020. IQ-TREE 2: New Models and Efficient Methods for Phylogenetic Inference in the Genomic Era. Mol Biol Evol 37:1530-1534.
150. Hoang DT, Chernomor O, von Haeseler A, Minh BQ, Vinh LS. 2018. UFBoot2: Improving the Ultrafast Bootstrap Approximation. Mol Biol Evol 35:518-522.
151. Pelliciari S, Dong MJ, Gao F, Murray H. 2021. Evidence for a chromosome origin unwinding system broadly conserved in bacteria. Nucleic Acids Res 49:7525-7536.
152. Nakamura A, Wada C, Miki K. 2007. Structural basis for regulation of bifunctional roles in replication initiator protein. Proc Natl Acad Sci U S A 104:18484-9.
153. Mirdita M, Schutze K, Moriwaki Y, Heo L, Ovchinnikov S, Steinegger M. 2022. ColabFold: making protein folding accessible to all. Nat Methods 19:679-682.
154. Ekundayo B, Bleichert F. 2019. Origins of DNA replication. PLoS Genet 15:e1008320.

AUTHOR BIOGRAPHIES

Théophile Niault

Théophile Niault holds a degree in life sciences from the Pierre and Marie Curie University in Paris, followed by a master's degree in molecular and cellular biology from Sorbonne University. He went on to pursue his Ph.D. in microbial genetics from Sorbonne University, where he worked as a member of the Bacterial Genome Plasticity Unit at Pasteur Institute, under the guidance of Professor Didier Mazel and Marie-Eve Val. Currently, Théophile is a post-doctoral fellow at the same laboratory, where he continues his research on the initiation of replication of the secondary chromosome of *Vibrio cholerae*.

Jakub Czarnecki

Jakub Czarnecki completed all his higher education at the University of Warsaw, Poland, where he received his PhD in molecular biology in 2015. He then continued to work at the same university for 2 years as an associate professor in Prof. Dariusz Bartosik's group, dealing with the organization of multi-partite genomes of bacteria of the genus Paracoccus, as well as the genetic basis of their methylotrophic metabolism. For the past five years, he has held a post-doc position in the laboratory of Professor Didier Mazel, studying the organization and replication of multi-partite genomes in bacteria from various taxonomic groups.

Morgan Lamberioux

Morgan Lamberioux graduated in pharmaceutical sciences from the University of Tours and holds a master's degree in molecular and cellular biology from the University of Paris. He is currently a PhD student at the Institut Pasteur and Sorbonne Université in microbial genetics within the Bacterial Genome Plasticity Unit under the supervision of Professor Didier Mazel. His PhD topic is the development of a killer conjugative plasmid as an innovative antibacterial.

Didier Mazel

Didier Mazel received his PhD in Genetics (1990) and is Professor at the Institut Pasteur, Paris. His projects are centered on an evolutionary mechanism in bacteria, in particular on the horizontal gene transfer and gene capture mechanisms. His group also works on the genome structure of bacteria which carry multiple chromosomes, such as *Vibrio cholerae*, the agent of cholera. He is the head of the Bacterial Genome Plasticity unit and was the director of the Genomes and Genetics department of the Institut Pasteur until 2018. He has published more than 130 articles on these topics. He has been elected a fellow of the American Academy of Microbiology, of the European Academy of Microbiology, and of Academia Europaea, and his work has been awarded several scientific prizes.

Marie-Eve Val

M.-E. Val is a French researcher in microbiology at the Institut Pasteur, Paris. She obtained an engineering degree in biotechnology at ESBS, Strasbourg, France, and completed her master's thesis at UMBI, Baltimore, USA, in 2003. She obtained her PhD in bacterial genetics at the Université de Paris-Saclay in 2008, focusing on *Vibrio* chromosome segregation and on the lysogeny mechanism of the cholera toxin phage. As a post-doctoral fellow, she joined Didier Mazel's team at the Institut Pasteur, where she studied the selective advantages of the two-chromosome genomic architecture of *Vibrio*, discovering a novel replication checkpoint mechanism. In 2013, she obtained a permanent research position from INSERM (National Institute of Health and Medical Research).

FIGURE LEGENDS

Figure 1. Genome organization of *Vibrionaceae* reference genomes. The reference strain of *E. coli* K-12 and 47 *Vibrionaceae* reference genomes were included in the tree. The concatenated sequences of 8 genes (*ftsK*, *gapA*, *gyrB*, *mreB*, *pyrH*, *recA*, *rpoA* and *topA*) were used for phylogenetic analysis as described by Jiang et al (147). Alignment was performed using MAFFT software (148). Phylogenetic tree was made with IQ-TREE multicore v2.0.3 (149). 286 DNA models were tested and GTR+F+R6 was selected as the best-fitting model to the IQ-TREE -m TESTNEW algorithm according to the Bayesian Information Criterion (BIC). The statistical data were derived from 1000 ultrafast bootstrap values and 1000 replicates of SH approximate likelihood ratio test (150). The raw data used to perform this analysis are in Table S1.

Figure 2. Replication regulated sequences are highly similar between *V. cholerae* and *E. coli*. A. Sequence alignment between *oriC* of *E. coli* (GenBank: U00096.3) and *ori1* from *V. cholerae* (GenBank: CP028827.1) reveals a highly similar organization. The *oriC* consists of a DNA unwinding element (DUE) containing single-stranded binding sites for DnaA (L, M and R elements and DnaA trios), as well as a DnaA assembly region (DAR) containing double-stranded binding sites for DnaA with strong boxes (R1, R2, and R4) and weak boxes (t1, R5, t2, I2, R3, I3). The IHF and FIS binding sequences are highlighted in green and yellow respectively. GATC Dam-methylation sites are in bold. **B.** Alignment of DARS2 site from *V. cholerae* and *E. coli*. Strong DnaA boxes (I, II, III, V) are highlighted in dark blue and weak DnaA boxes (V-c, V-b, V-a) are in light blue. FIS binding site is indicated in yellow. Alignments and annotations were retrieved from (30, 31, 95, 151).

Figure 3. Schematic of the origin organization of iteron plasmids and Chr2 of *V. cholerae*. Initiator genes are displayed in purple and initiator binding sites (iterons and inverted repeats) in green. The 29/39m RctB binding sites (specific to Chr2) are shown in red. DnaA binding sites are shown in light blue. The incompatibility regions (*inc*) and DNA

unwinding elements (DUE) are indicated. These organization schemes are in scale. The replicon sequences were retrieved from the NCBI database (GenBank: pSC101: X01654.1, pPS10: X58896.1, R6K: LT827129.1, F: AP001918.1, RK2: CP116242.1, P1: OP279344.1, Chr2: CP028828.1).

Figure 4. Domain II and III from RctB are structural homologues to WH1 and WH2 from Rep proteins. A. Pi_{R6K} , **B.** $RepA_{pPS10}$, **C.** $RepE_{F}$, **D.** $RctB_{Chr2}$. Rep proteins dimerize through their WH1 domain, RctB dimerize through its domain II. RepE and RctB dimer structures were retrieved from PDB (2Z9O and 5UBF respectively) (52, 152). Pi_{R6K} and $RepA_{pPS10}$ dimer structures have been predicted using ColabFold v1.5.2 (153) (Fig. S1). Initiator sequences were retrieved from replicon sequences present on the NCBI database (pPS10: X58896.1, R6K: LT827129.1)

Figure 5. The RctB initiator is organized into four structural domains. A. RctB is a 658-residue protein that contains four structural domains I II III and IV. Domains I, II and III are all involved in DNA binding via an HTH motif. Domains II and III are structurally similar to the WH1 and WH2 domains of iteron plasmid initiators. Domain IV allows oligomerization and is dedicated to regulating Chr2 initiation. **B.** Predicted structure of RctB using ColabFold v1.5.2 (153) (Fig. S1). **C.** Structure of RctB with amino acids involved in DNA binding in dark red (52). **D.** Schematic depicting the binding of RctB to the iteron array (six iterons) of the *V. cholerae* Chr2 origin of replication. Note that the precise conformation of RctB to its various sites remains an open question. The same color code as in panel A is used throughout the figure.

Figure 6. Model for replication origin opening in Chr1 and Chr2. **A.** *ori1* : The origin of replication of Chr1 is a 245-bp-long sequence. It contains three types of predicted DnaA binding sites (30, 151) : Strong double-stranded sites (dark blue: R1, R2, R4); Weak double-stranded sites (light blue: T1, R5, T2, I1, I2, C3, R3, C2, I3, C1); Single-stranded sites inside the DNA unwinding element (grey: DUE, red: L, M, R elements, orange: DnaA trios). *ori2min*

: The minimal Chr2 origin of replication is 258bp long and contains a strong DnaA box, six regularly interspaced repeats of 12mer (iterons), an IHF binding site (IBS), and six tetranucleotide ATCA repeats inside the DUE (59, 60). **B.** DnaA and RctB loopback models adapted from (60, 61, 154). DnaA and RctB initiators are shown in yellow and purple, respectively. For clarity, the oligomerization domains of DnaA (domain I) and RctB (domain IV) are not shown. Association of DnaA with ATP is mandatory for binding to weak DnaA boxes (dark green circles). For binding to strong DnaA boxes, DnaA can be associated with either ATP or ADP (light green circles). IHF is shown in pink, DUE open ssDNA is shown in grey. DnaA binding sites are displayed in the same color code as panel A.

Figure 7. Chr2 initiation is activated by *crtS* replication, the timing of which can be modulated by the distance of *crtS* from the Chr1 origin. Left panel: Schematic representing the replicative state of Chr1 (red) when Chr2 (green) initiation is triggered. The blue rectangle indicates the location of *crtS* when replicated. **Middle panel:** Schematic representation of marker frequency analysis (MFA) of exponentially growing cultures with Log2 of the number of reads plotted against their relative position on Chr1 (red) and Chr2 (green). The blue dashed lines indicate the number of reads of loci where *crtS* is located ($crtS_{VC23}$, $crtS_{WT}$, $crtS_{VC963}$, $crtS_{VC2238}$). The positions of *ori1* and *ori2* are set to 0 for a better visualization of the bidirectional replication. The difference between the number of reads at *ter1* and *ter2* is shaded in gray and indicated by a double arrow. Figure adapted and based on real sequencing data from published work (15). **Right panel:** Effect of *crtS* relocation on Chr1 and Chr2 termination synchrony.

Figure 8. Model for coordination of replication between Chr1 and Chr2 by *crtS*. The cooperative binding of RctB to the fully methylated iteron array causes DNA opening and RctB oligomerization on the ssDNA DUE (green arrow). RctB binding to the 29/39m sites inhibits replication initiation at *ori2* by intra-molecular handcuffing and represses its own transcription at the 29m (red arrows). Upon replication, *crtS* triggers *ori2* initiation by counteracting the inhibitory effect of the 29/39m sites (blue arrows). The four domains of

RctB are represented (I-IV). RctB dimers (domain II-interface) are monomerized by the DnaK/J chaperones. RctB monomers cooperatively bind to the iteron array. RctB binding to the 29/39m requires domain IV mediated interactions. Lrp enhances RctB binding to *crtS*. RctB binding sites are indicated : iteron array (green), 29m and 39m (red) and *crtS* (blue). The iterons present in the *inc* region have been omitted for clarity. Positive and negative regulations are represented by arrows associated with (+) and (-), respectively.

Figure 9. *V.* cholerae chromosome segregation and divisome assembly. The single flagellum of *V. cholerae* is shown to be localized at the old pole, while Chr1 and Chr2 are arranged longitudinally with their *ter* regions indicated by broken lines. 3C data is represented by dashed arcs, showing interactions between the left and right replichores of Chr2. Inter-chromosomal contacts are also shown, with *ori2* in proximity to *crtS*, as well as the *ter1* and *ter2* regions. The partitioning systems (ParAB-*parS*) of each chromosome are represented by colored halos around the replication origins. **(I)** In nascent cells, HubP is present at the old pole along with *ori1* and the ParAB1-*parS1* partition complex. All cell division proteins (early and late) localize to the new pole along with *ter1*. **(II)** As the cell cycle progresses to ~50%, cells elongate and early cell division proteins move to mid-cell, forming a pre-divisional Z-ring. Late cell division proteins remain at the new pole where HubP starts accumulating. A duplicated copy of *ori1* complexed with ParAB1 is recruited by HubP to the new pole. The duplication of *crtS* has triggered *ori2* replication. The duplicated copies of *ori2* moved to the ¼ - ¾ positions of the cell. **(III)** At ~80% of the cell cycle, all division proteins have migrated to mid-cell, assembling into a tighter Z-ring. The *ter2* are already segregated while *ter1* are still at the future division site. **(IV)** At 90% of the cell cycle, constriction begins and HubP is evenly distributed at both poles. *ter1* are segregated by FtsK anchored to the closing septum.

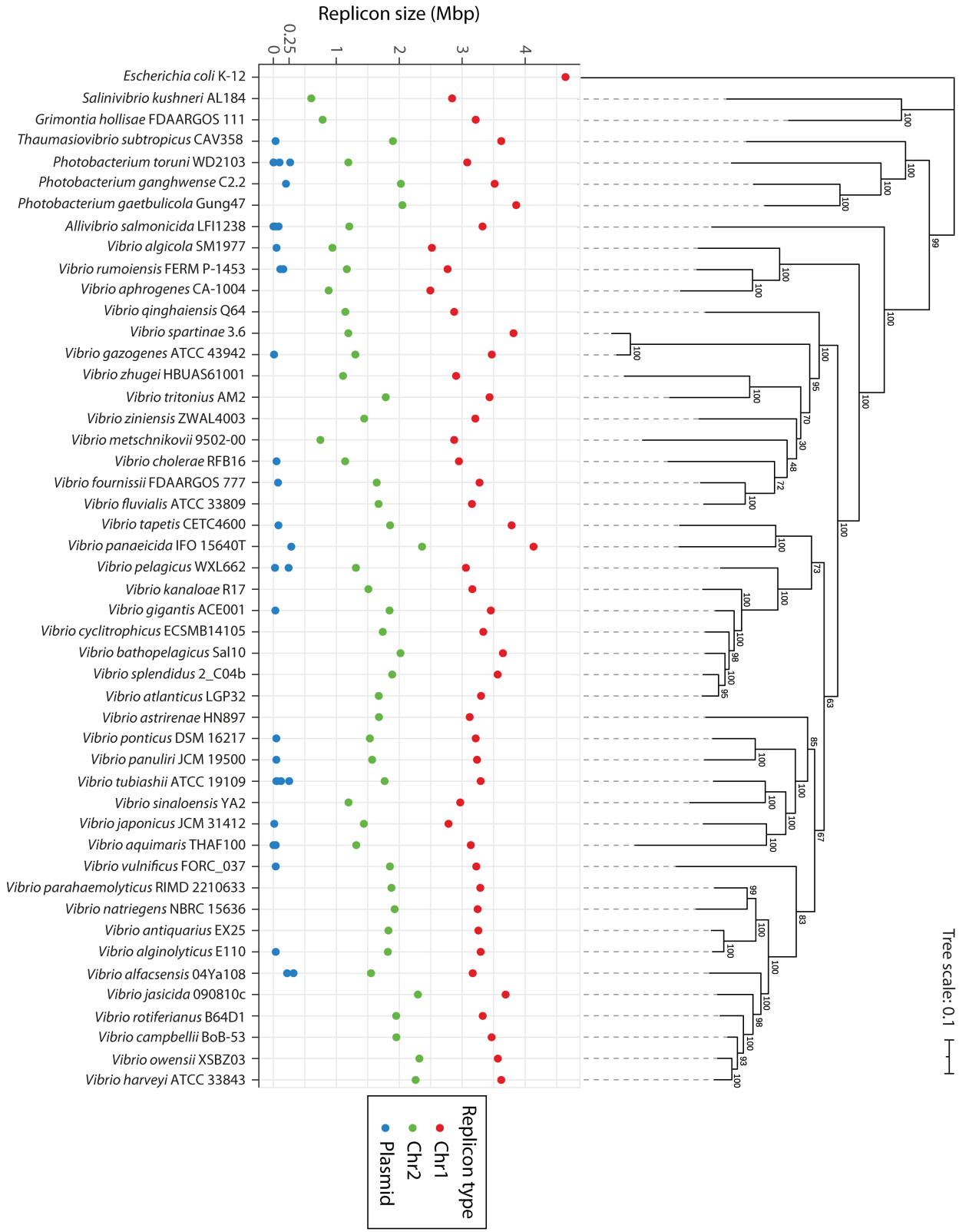
Replicon size (Mbp)
0
0.25
1
2
3
4
Escherichia coli K-12
Salinivibrio kushneri AL184
Grimontia hollisae FDAARGOS 111
Thaumasiovibrio subtropicus CAV358
Photobacterium toruni WD2103
Photobacterium ganghwense C2.2
Photobacterium gaetbulicola Gung47
Allivibrio salmonicida LFI1238
Vibrio algicola SM1977
Vibrio rumoiensis FERM P-1453
Vibrio aphrogenes CA-1004
Vibrio qinghaiensis Q64
Vibrio spartinae 3.6
Vibrio gazogenes ATCC 43942
Vibrio zhugei HBUAS61001
Vibrio tritonius AM2
Vibrio ziniensis ZWAL4003
Vibrio metschnikovii 9502-00
Vibrio cholerae RFB16
Vibrio fournissii FDAARGOS 777
Vibrio fluvialis ATCC 33809
Vibrio tapetis CETC4600
Vibrio panaeicida IFO 15640T
Vibrio pelagicus WXL662
Vibrio kanaloae R17
Vibrio gigantis ACE001
Vibrio cyclitrophicus ECSMB14105
Vibrio bathopelagicus Sal10
Vibrio splendidus 2_C04b
Vibrio atlanticus LGP32
Vibrio astrirenae HN897
Vibrio ponticus DSM 16217
Vibrio panuliri JCM 19500
Vibrio tubiashii ATCC 19109
Vibrio sinaloensis YA2
Vibrio japonicus JCM 31412
Vibrio aquimaris THAF100
Vibrio vulnificus FORC_037
Vibrio parahaemolyticus RIMD 2210633
Vibrio natriegens NBRC 15636
Vibrio antiquarius EX25
Vibrio alginolyticus E110
Vibrio alfacsensis 04Ya108
Vibrio jasicida 090810c
Vibrio rotiferianus B64D1
Vibrio campbellii BoB-53
Vibrio owensii XSBZ03
Vibrio harveyi ATCC 33843
Tree scale: 0.1
Replicon type
Chr1
Chr2
Plasmid

Figure 1

Figure 2

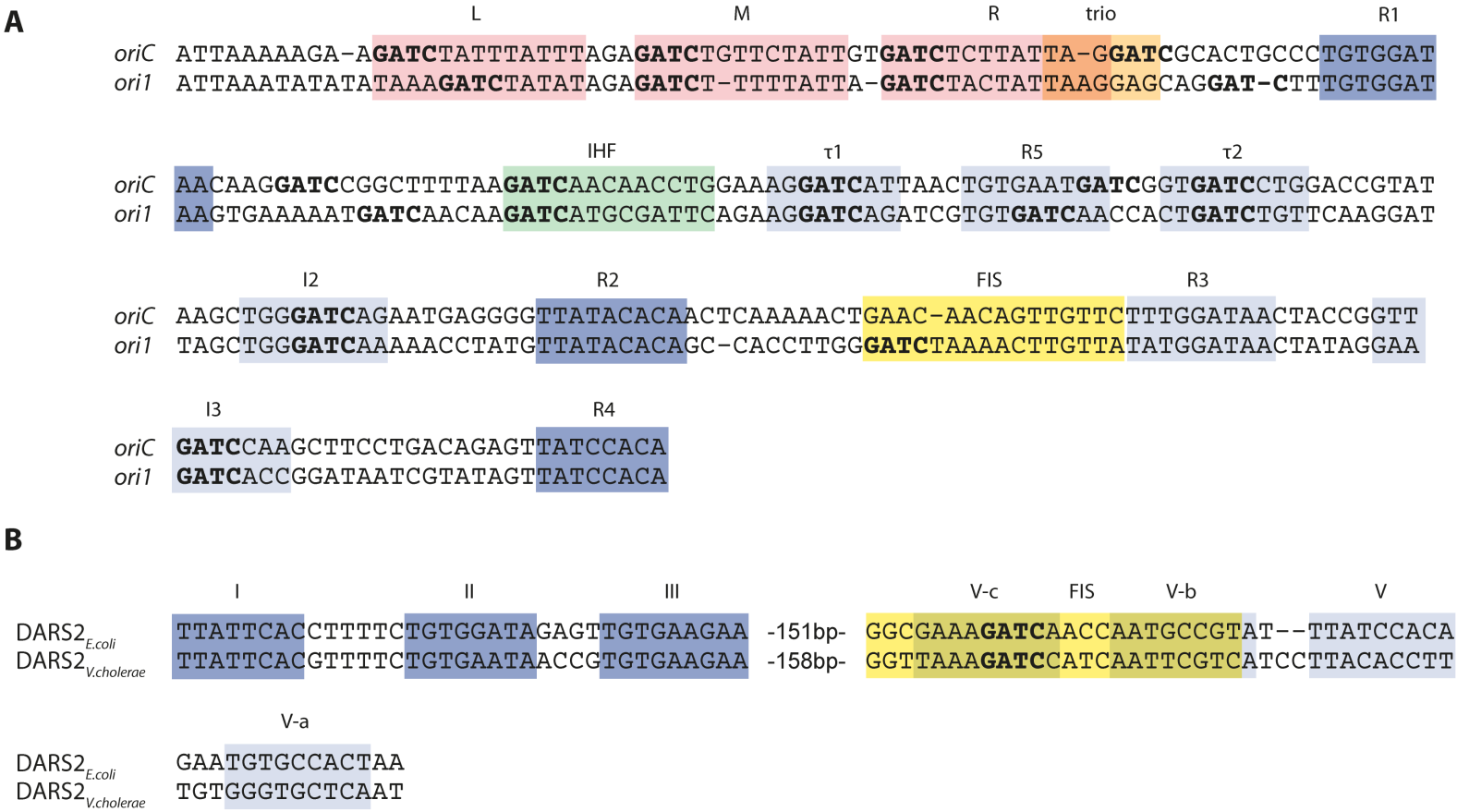
A
L
M
R
trio
R1
oriC ATTAAAAAGA-AGATCTATTTATTTAGAGATCTGTTCTATTGTGATCTCTTATTA-GGATCGCACTGCCCTGTGGAT
ori1 ATTAAATATATATAAAGATCTATATAGAGATCT-TTTTATTA-GATCTACTATTAAGGAGCAGGAT-CTTTGTGGAT
IHF
τ1
R5
τ2
oriC AACAAGGATCCGGCTTTTAAGATCAACAACCTGGAAAGGATCATTAACTGTGAATGATCGGTGATCCTGGACCGTAT
ori1 AAGTGAAAAATGATCAACAAGATCATGCGATTCAGAAGGATCAGATCGTGTGATCAACCACTGATCTGTTCAAGGAT
I2
R2
FIS
R3
oriC AAGCTGGGATCAGAATGAGGGGTTATACACAACTCAAAAACTGAAC-AACAGTTGTTCTTTGGATAACTACCGGTT
ori1 TAGCTGGGATCAAAAACCTATGTTATACACAGC-CACCTTGGGATCTAAAACTTGTTATATGGATAACTATAGGAA
I3
R4
oriC GATCCAAGCTTCCTGACAGAGTTATCCACA
ori1 GATCACCGGATAATCGTATAGTTATCCACA
B
I
II
III
V-c
FIS
V-b
V
DARS2E.coli TTATTCACCTTTTCTGTGGATAGAGTTGTGAAGAA -151bp- GGCGAAAGATCAACCAATGCCGTAT--TTATCCACA
DARS2V.cholerae TTATTCACGTTTTCTGTGAATAACCGTGTGAAGAA -158bp- GGTTAAAGATCCATCAATTCGTCATCCTTACACCTT
V-a
DARS2E.coli GAATGTGCCACTAA
DARS2V.cholerae TGTGGGTGCTCAAT

Figure 3

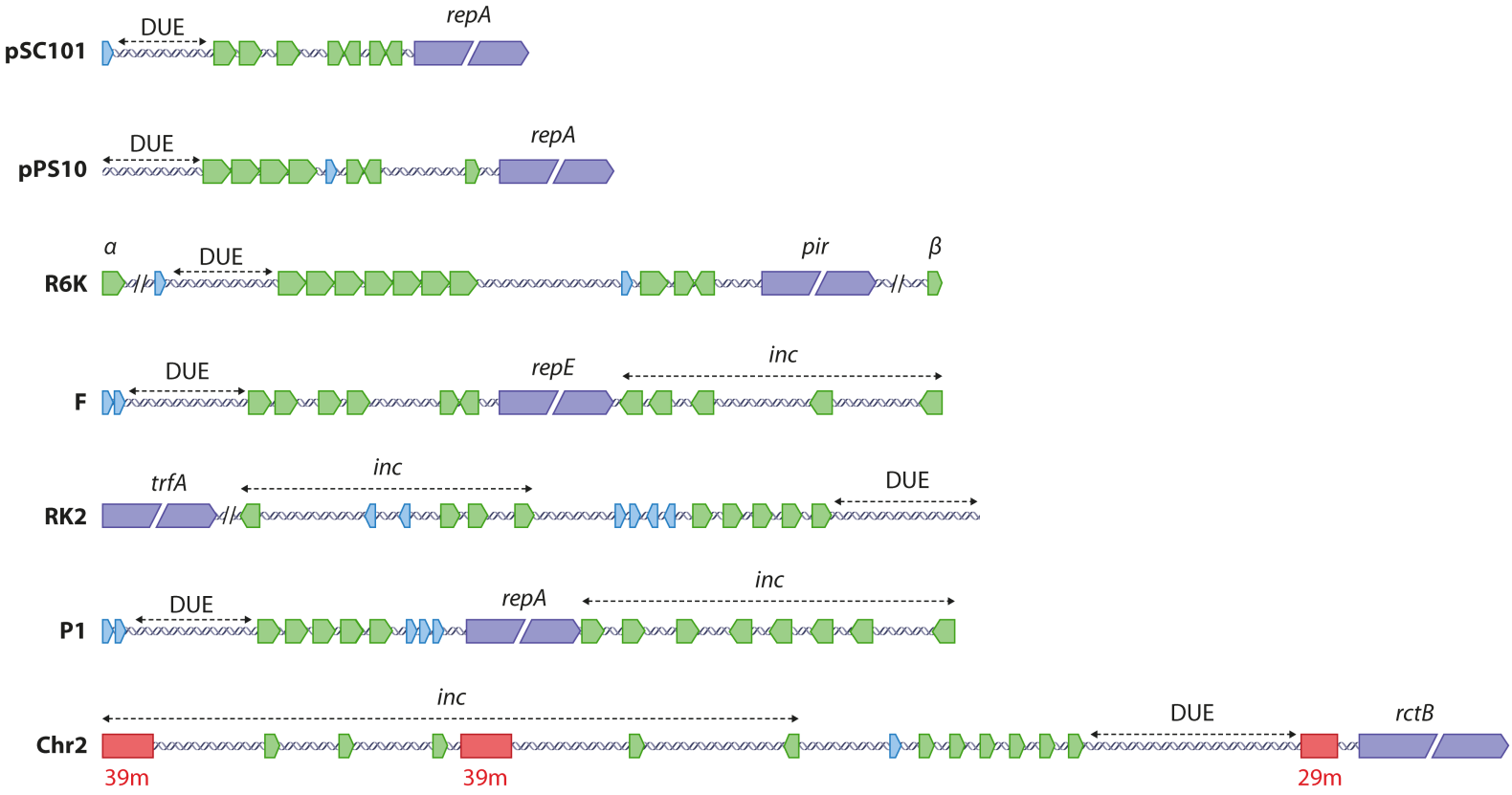
pSC101
DUE
repA
pPS10
DUE
repA
R6K
α
DUE
pir
β
F
DUE
repE
inc
RK2
trfA
inc
DUE
P1
DUE
repA
inc
Chr2
inc
39m
39m
DUE
29m
rctB

Figure 4

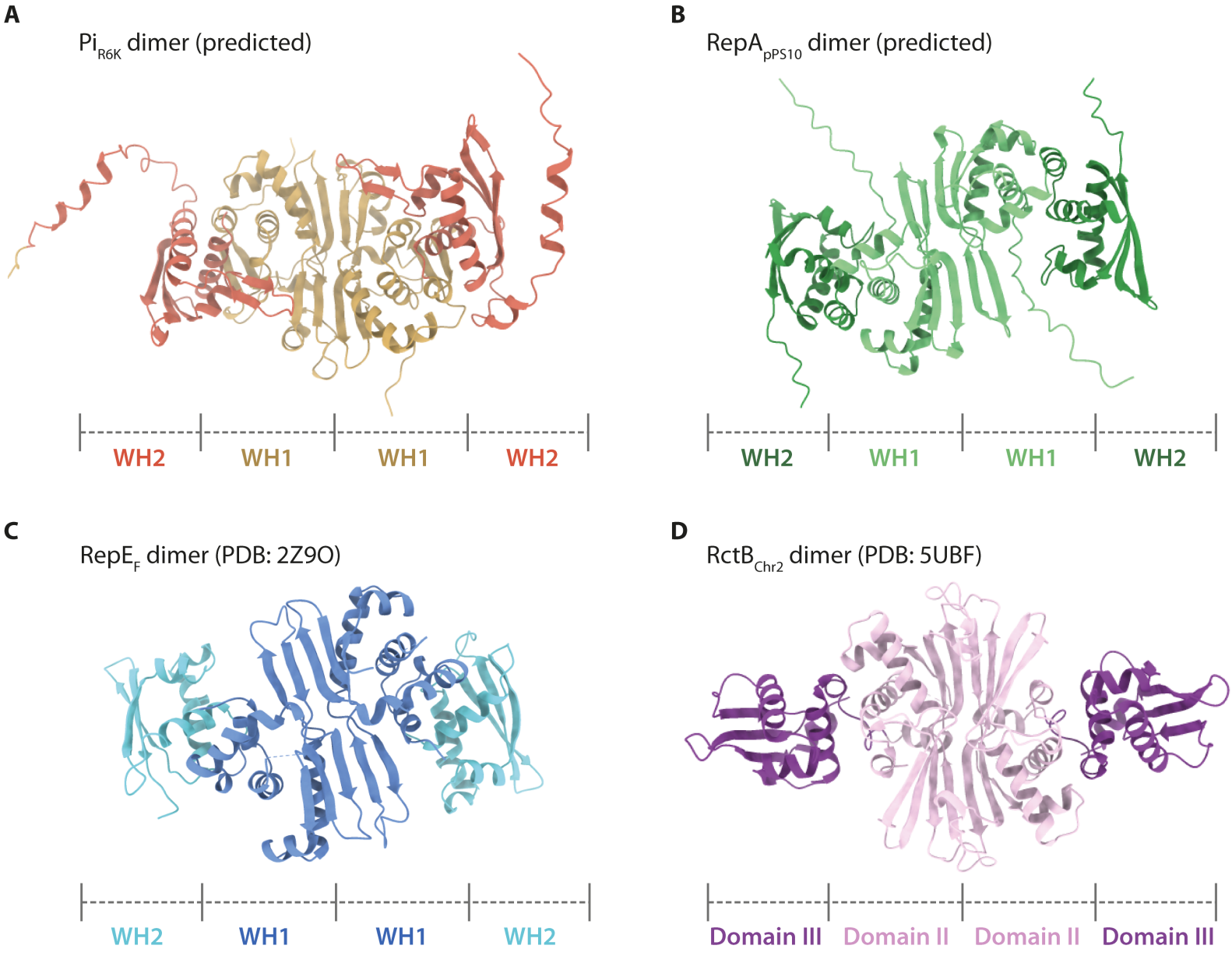
A
Pi$_{R6K}$ dimer (predicted)
WH2
WH1
WH1
WH2
B
RepA$_{pPS10}$ dimer (predicted)
WH2
WH1
WH1
WH2
C
RepE$_{F}$ dimer (PDB: 2Z9O)
WH2
WH1
WH1
WH2
D
RctB$_{Chr2}$ dimer (PDB: 5UBF)
Domain III
Domain II
Domain II
Domain III

Figure 5

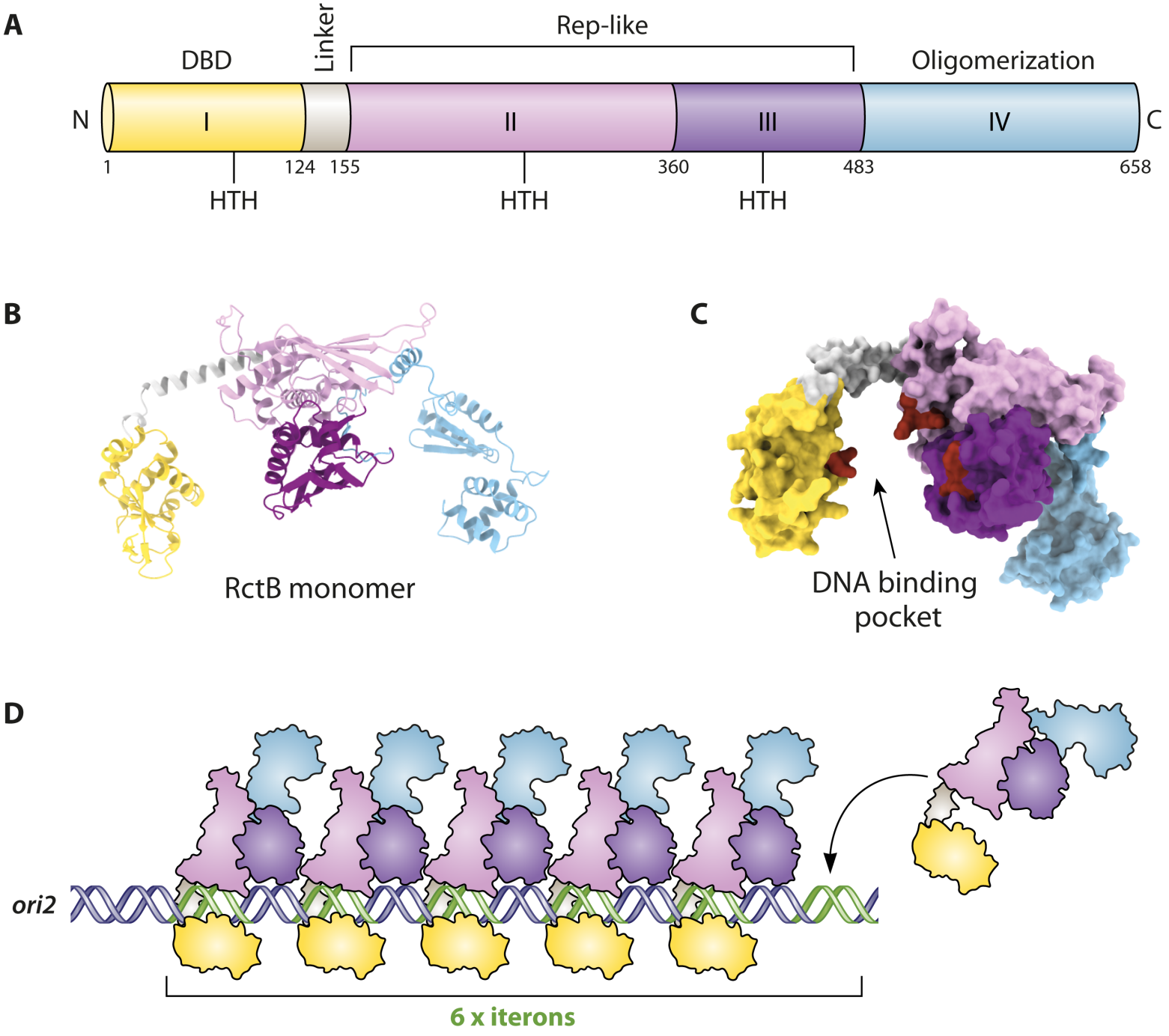
A
DBD
Linker
Rep-like
Oligomerization
N
I
II
III
IV
C
1
124
155
360
483
658
HTH
HTH
HTH
B
RctB monomer
C
DNA binding
pocket
D
ori2
6 x iterons

Figure 6

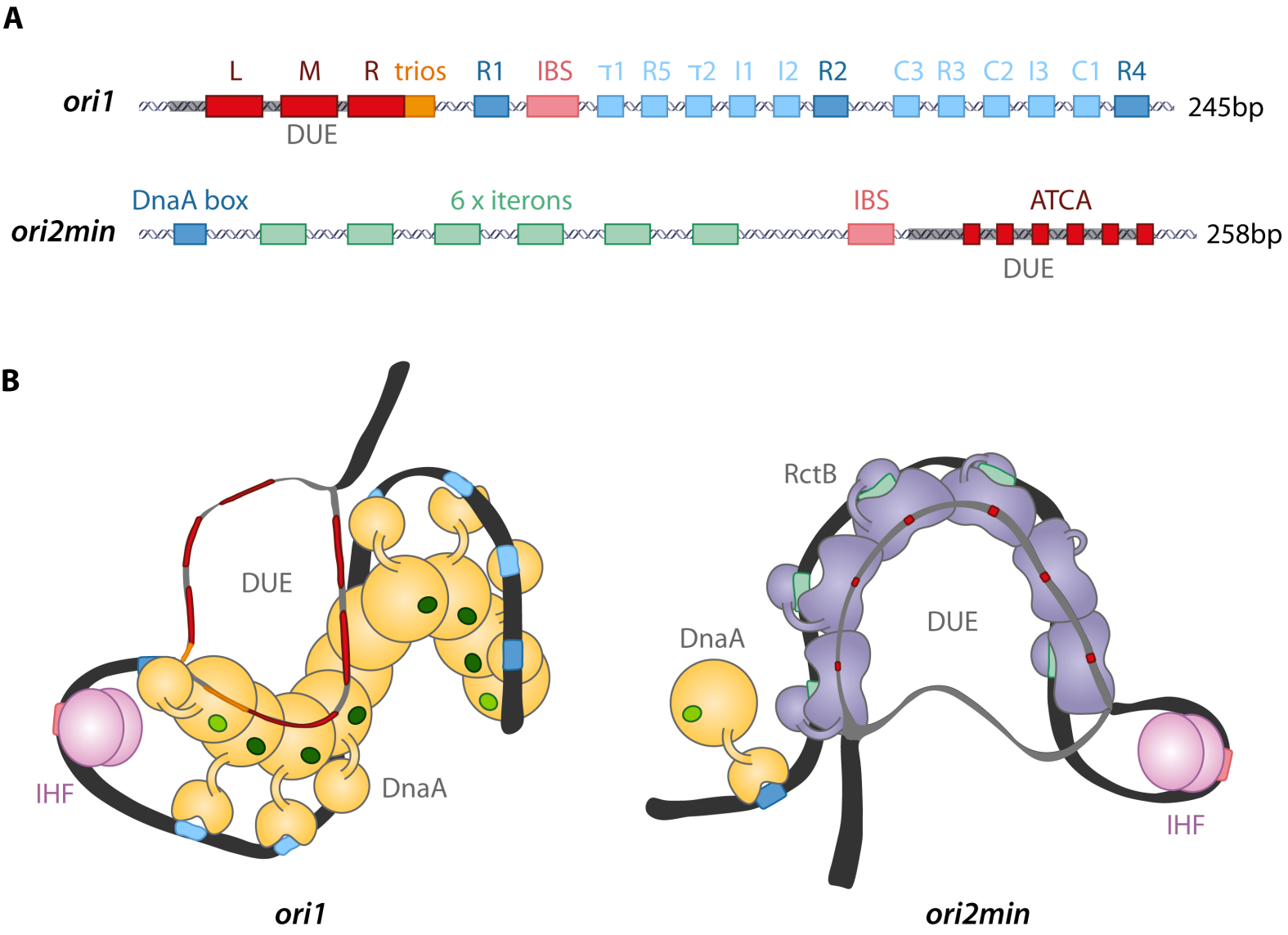
A
ori1
L
M
R
trios
R1
IBS
τ1
R5
τ2
I1
I2
R2
C3
R3
C2
I3
C1
R4
DUE
245bp
ori2min
DnaA box
6 x iterons
IBS
ATCA
DUE
258bp
B
DUE
IHF
DnaA
ori1
RctB
DnaA
DUE
IHF
ori2min

Figure 7

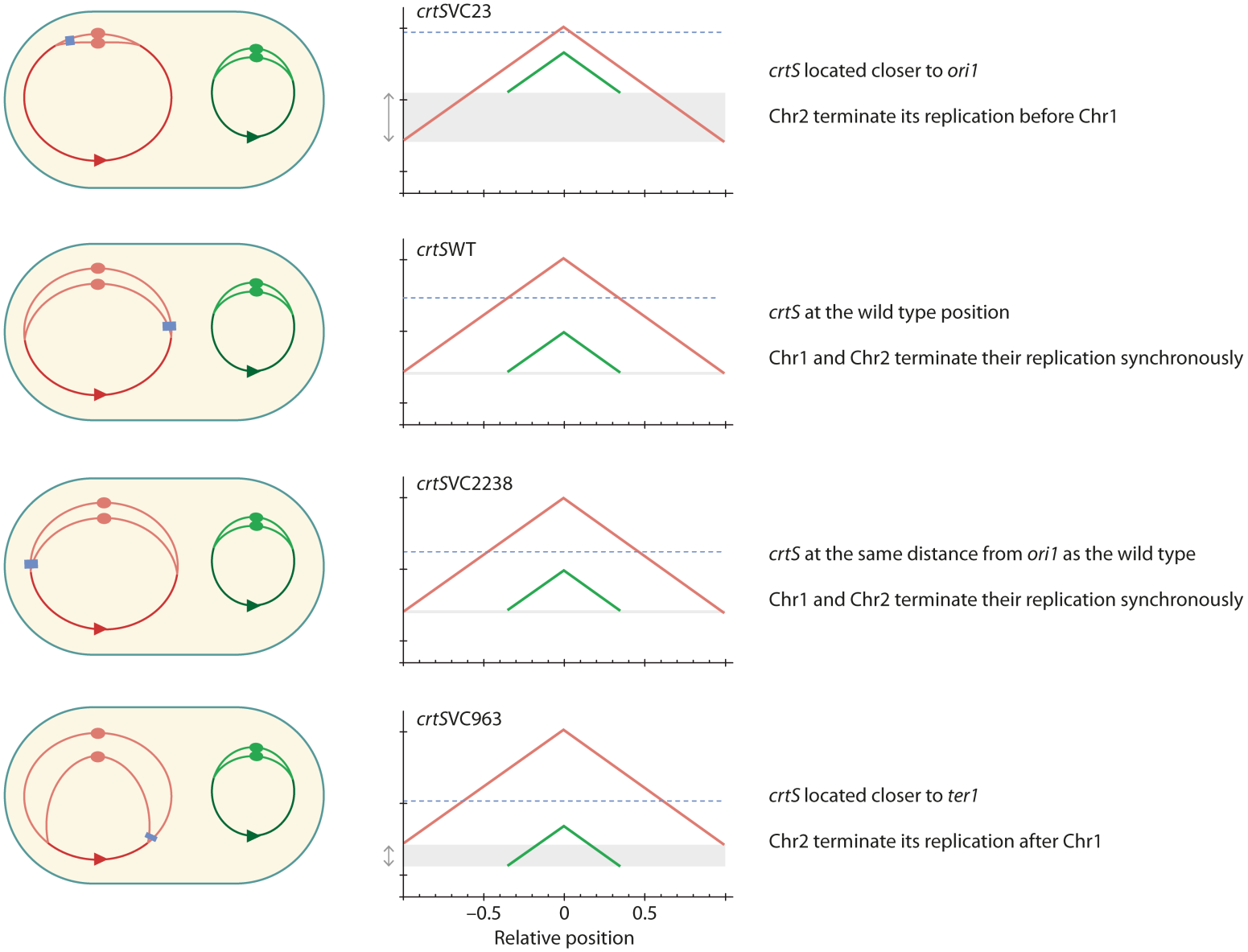
crtSVC23
crtS located closer to ori1
Chr2 terminate its replication before Chr1
crtSWT
crtS at the wild type position
Chr1 and Chr2 terminate their replication synchronously
crtSVC2238
crtS at the same distance from ori1 as the wild type
Chr1 and Chr2 terminate their replication synchronously
crtSVC963
crtS located closer to ter1
Chr2 terminate its replication after Chr1
−0.5
0
0.5
Relative position

Figure 8

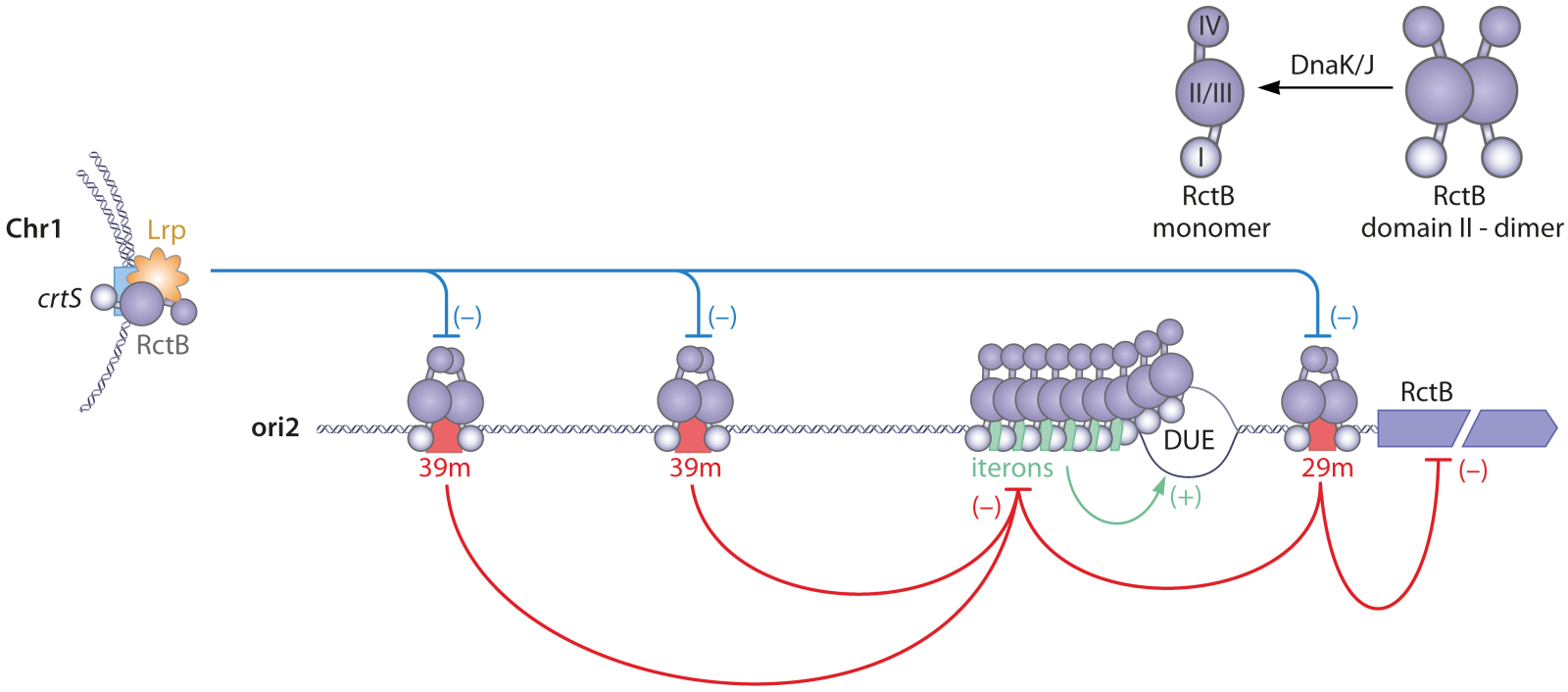
IV
II/III
I
DnaK/J
RctB
monomer
RctB
domain II - dimer
Chr1
Lrp
crtS
RctB
(–)
(–)
(–)
ori2
39m
39m
iterons
DUE
(+)
(–)
29m
RctB
(–)

Figure 9

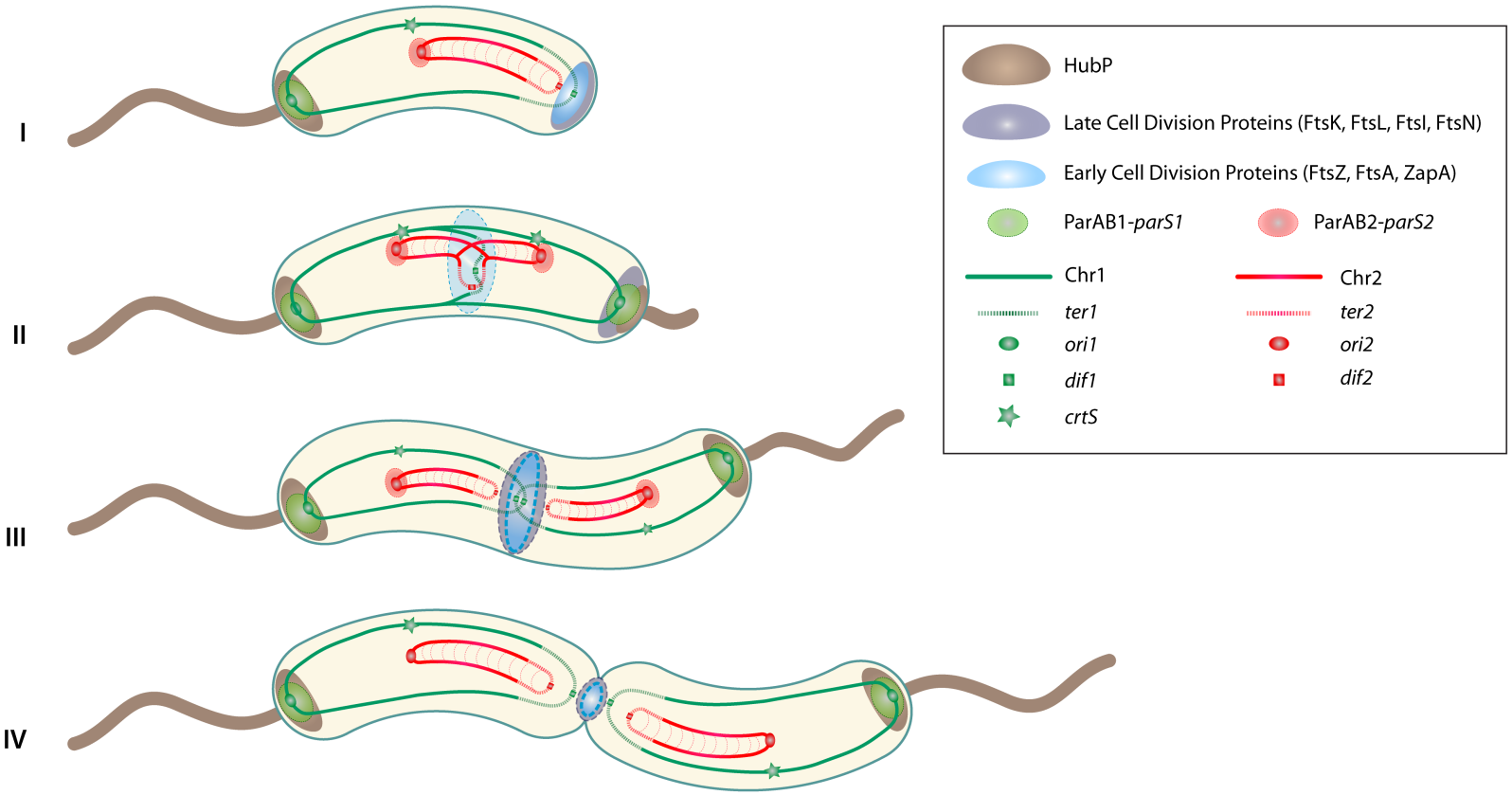
I
II
III
IV
HubP
Late Cell Division Proteins (FtsK, FtsL, FtsI, FtsN)
Early Cell Division Proteins (FtsZ, FtsA, ZapA)
ParAB1-parS1
ParAB2-parS2
Chr1
Chr2
ter1
ter2
ori1
ori2
dif1
dif2
crtS